Solid Oxide Fuel Cell Manufacturing Cost Model:

Simulating Relationships between Performance, Manufacturing, and Cost of Production

Final Report to:
National Energy Technology Laboratory
U.S. Department of Energy

April 2, 2004

DOE Cooperative Agreement Number: DE-FC26-02NT41568

Report prepared by: TIAX LLC

Authors:
Eric J. Carlson
Yong Yang
Chandler Fulton

Reference D0058

ABSTRACT

The successful commercialization of fuel cells will depend on the achievement of competitive system costs and efficiencies. System cost directly impacts the capital equipment component of cost of electricity (COE) and is a major contributor to the O&M component. The replacement costs for equipment (also heavily influenced by stack life) is generally a major contributor to O&M costs.

In this project, we worked with the SECA industrial teams to estimate the impact of general manufacturing issues of interest using an activities-based cost model for anode-supported planar SOFC stacks with metallic interconnects. An earlier model developed for NETL for anode supported planar SOFCs was enhanced by linkage to a performance/thermal/mechanical model, by addition of Quality Control steps to the process flow with specific characterization methods, and by assessment of economies of scale. The 3-dimensional adiabatic performance model was used to calculate the average power density for the assumed geometry and operating conditions (i.e., inlet and exhaust temperatures, utilization, and fuel composition) based on publicly available polarization curves.

The SECA teams provided guidance on what manufacturing and design issues should be assessed in this Phase I demonstration of cost modeling capabilities. We considered the impact of the following parameters on yield of cost: layer thickness (i.e., anode, electrolyte, and cathode) on cost and stress levels, statistical nature of ceramic material failure on yield, and Quality Control steps and strategies.

In this demonstration of the capabilities of the linked model, only the active stack (i.e., anode, electrolyte, and cathode) and interconnect materials were included in the analysis. Factory costs are presented on an area and kilowatt basis to allow developers to extrapolate to their level of performance, stack design, materials, seal and system configurations, and internal corporate overheads and margin goals.

TABLE OF CONTENTS

ABSTRACT **2**

TABLE OF CONTENTS **3**

LIST OF TABLES **5**

LIST OF FIGURES **6**

1. EXECUTIVE SUMMARY **8**

2. INTRODUCTION **10**

2.1. SECA PROGRAM 10
2.2. 1999 FETC SOFC COST ANALYSIS OVERVIEW 11
2.3. 2003 NETL SOFC COST ANALYSIS PROJECT OBJECTIVES AND APPROACH 11
2.3.1. Project Objectives *11*
2.3.2. Project Approach and Deliverables *12*
2.3.3. Cost Model Benefits to the SECA Industrial Teams *13*
2.3.4. SECA Team Feedback *14*

3. 1999 COST RESULTS **16**

3.1. 1999 COST MODEL ASSUMPTION 16
3.1.1. Stack Description *16*
3.1.2. Process Assumptions *17*
3.2. 1999 MANUFACTURING COST MODEL RESULTS 19

4. MODELING METHODOLOGY **20**

4.1. PERFORMANCE/THERMAL/MECHANICAL MODEL APPROACH 20
4.1.1. Background *20*
4.1.2. Methodology *20*
4.2. MANUFACTURING COST MODEL DESCRIPTION 24
4.2.1. Cost Definition *25*
4.2.2. Cost Modeling Methodology *26*
4.2.3. Databases *27*
4.2.4. Process Flow *27*
4.2.5. Materials *28*
4.3. QUALITY CONTROL 31
4.3.1. Inspection Accuracy Level *32*
4.3.2. Yield vs. EEA Defective Rate *33*

4.4. ECONOMIES OF SCALE 34
4.4.1. Objective 34
4.4.2. Methodology 34
4.5. SENSITIVITY ANALYSIS AND MONTE CARLO SIMULATION 37
4.6. 2003 MODEL ASSUMPTION SUMMARY 38
4.6.1. Stack Components 38
4.6.2. Repeat Unit Layer Thickness 38
4.6.3. Related Manufacturing Data 40
4.6.4. Baseline Processes 40
4.6.5. 2003 Assumption vs. 1999 Assumption 42
5. RESULTS AND DISCUSSION 43
5.1. BASELINE COST RESULTS 43
5.1.1. Performance/Thermal/Mechanical Model 43
5.1.2. Manufacturing Costing 48
5.2. ECONOMIES OF SCALE 54
5.3. QUALITY CONTROL ANALYSIS RESULTS 58
5.3.1. Inspection Accuracy Level 58
5.3.2. Stack Cost vs EEA Defective Rate 58
5.4. FUTURE TOPICS FOR COST MODELING 59
6. CONCLUSIONS 61
6.1. PERFORMANCE/THERMAL/MECHANICAL MODEL DISCUSSION 61
7. REFERENCES 63
8. APPENDIX 64
8.1. EEA AND STACK PARAMETERS 64
8.2. COMMON SOFC MANUFACTURING PROCESSES 65
8.3. ECONOMIES OF SCALE PARAMETERS 70

LIST OF TABLES

Table 1 1999 Stack Description ... 16
Table 2 1999 Manufacturing Cost Breakdown on $/kW Basis ... 19
Table 3 Key Model Assumptions, Primary Uses, and Outputs ... 21
Table 4 Weibull Parameters for SOFC Material Failure Statistics (Data from ORNL) ... 23
Table 5 Anode Layer Materials and Binders ... 28
Table 6 Cathode Layer Materials and Binders ... 29
Table 7 Electrolyte Layer Material and Binders ... 29
Table 8 Sample Cost Model Calculations Sheet ... 31
Table 9 Scenarios I & II ... 33
Table 10 Manufacturing Process Scale-Up by Volume ... 35
Table 11 Material Cost Scaled Up by Volume ... 36
Table 12 2003 Repeat Unit Layer Thickness ... 39
Table 13 Production Parameters ... 40
Table 14 Manufacturing Cost Model Assumptions – 2003 vs. 1999 ... 42
Table 15 Range of Layer Thicknesses Simulated ... 43
Table 16 Predicted Power Density for selected Combinations of Layer Thicknesses ... 44
Table 17 Predicted Peak Stresses and Material Yields for Co-Fired Processing ... 47
Table 18 Predicted Peak Stresses and Material Yields for Multi-Fired Processing ... 48
Table 19 Product Specifications ... 64

LIST OF FIGURES

Figure 1 Project Overview 13
Figure 2 Description of Phase I Year 1 Tasks 13
Figure 3 Schematic Baseline Planar SOFC Repeat Unit Structure 16
Figure 4 1999 Manufacturing Cost Model Multi-Fired Process Flow 18
Figure 5 1999 Manufacturing Cost Model Co-Fired Process Flow 18
Figure 6 1999 Manufacturing Cost Break Down on an Area Basis 19
Figure 7 Typical Geometry of Finite Element Simulations for Performance Modeling 21
Figure 8 Model Structure 21
Figure 9 Failure Probability Curves as a Function of Peak Tensile Stress (Data from ORNL) .. 24
Figure 10 Manufacturing Cost Model Schematic 25
Figure 11 Costs Structure 26
Figure 12 Manufacturing Cost Model Database Diagram 27
Figure 13 Co-Fired Process Flow 28
Figure 14 Design Product Material Calculation Flow 30
Figure 15 Three EEA's Inspection Processes 32
Figure 16 Quality Control Process Sequence 32
Figure 17 Quality Control Process Sequent 34
Figure 18 Sample Sensitivity Chart 37
Figure 19 Sample Frequency Chart 38
Figure 20 Manufacturing Cost Model Cost Structure 38
Figure 21 Co-Fired Process Flow Chart 41
Figure 22 Multi-Fired Process Flow Chart 42
Figure 23 Power Density Distribution of 10 cm Cross-Flow Cell with Nominal Layer Thicknesses and Baseline Operating Conditions, with an Average Power Density of 470 mW/cm^2 43
Figure 24 Variations of Cell-Average Power Density at Fixed Nominal Cathode Thickness, Under Baseline Operating Conditions 45
Figure 25 Comparison of Predicted Power Density Values with Best Fit Functional Form, at Fixed Nominal Cathode Thickness 46
Figure 26 2003 Total Stack Factory Cost ($\$/m^2$) 49
Figure 27 2003 Total Stack Factory Cost ($/KW) 49
Figure 28 Total Stack Factory Cost Comparison 2003 vs. 1999 50
Figure 29 Total Stack Factory Cost by Layer Comparison 2003 vs. 1999 50
Figure 30 Material Costs Breakdown 51
Figure 31 Material Cost Comparison with 1999 Model 52
Figure 32 Process Cost by Layer Comparison with 1999 Model 52
Figure 33 Process Cost by Step Comparison with 1999 Model 52
Figure 34 Multi-Fired Process Sensitivity Analysis 53
Figure 35 Forecast Frequency Charge from Monte Carlo Simulation 54

Figure 36 Breakdown Stack Costs as a Function of Production Volume ($\$/m^2$) 55
Figure 37 Stack Costs and Cost Reduction Rate as a Function of Production Volume ($\$/m^2$) 55
Figure 38 Process and Material Costs as a Function of Productions Volume ($\$/m^2$) 56
Figure 39 Capital Equipment Cost as a Function of Production Volume (1 Million $) 57
Figure 40 Scenario I & II Total Cost Comparison 58
Figure 41 Stack Cost vs. Percentage of Defective EEAs 59
Figure 42 Ball Milling Process 65
Figure 43 Tape Casting Machine Main Structure 66
Figure 44 Fully Automatic Screen Printing Batch Process Flow 67
Figure 45 Roll Forming Process Flow 68

1. EXECUTIVE SUMMARY

We have developed a computational manufacturing model that simulates the relationships between the performance of the technology, the potential operating window for the manufacturing processes, and the production costs of the product. This activity based manufacturing cost model was designed to address the primary goal of the SECA program by establishing a tool which provides guidance to the DOE and SECA development teams on system design and manufacturing process selection.

After discussions with the SECA industrial teams and NETL, the following topics were selected to demonstrate the benefits of the cost modeling tool, including:

- Update a 1999 cost model of anode supported planar SOFC stack technology with 2003 material and process data. A performance/mechanical/thermal developed for NETL was used to calculate average power densities for the assumed operating conditions, constraints, and stack design, while satisfying target fuel utilization values.
- Incorporate steps and equipment required for quality control (QC) into the process flow.
- Assess the effect of varying anode, electrolyte, and cathode thickness on power density, maximum stresses, and yield, the latter by comparison of stress distributions with failure curves for the ceramic materials
- Assess the impact of scaling up production volume from 5 MW to 250 MW on the cost of the stack while identifying drivers for cost reduction.

The analysis was based on the stack design assumed in the 1999 study as a baseline to provide continuity. Conventional SOFC materials (i.e., nickel cermet anode, 8 YSZ electrolyte, and LSM cathode) with nominal anode/electrolyte/cathode thickness of 700/10/50 microns respectively were used to develop a bill-of-materials. A rolled formed ferritic stainless steel was assumed for the interconnect, however, a stabilizing conductive coating was not used. In this demonstration, we focused only on the active materials and the interconnect. The seals and manifolds were excluded from this cost analysis.

For a fuel (reformate) utilization of 85%, cell voltage of 0.7 V, maximum temperature gradient of 150^{o}C across the stack, and maximum stack temperature of 800^{o}C, the performance model calculated a baseline average power density of 470 mW/cm^{2}. The model parameters were previously calibrated using single cell kinetic data from the literature. For these operating conditions, the stress conditions resulted in less than 5% cracking of the materials based failure data from ORNL. Power density increased when using thinner ceramic layers in the cell reaching a maximum of 570 mW/cm^{2} at the minimum thickness allowed for each layer.

The updated analysis of stack cost showed that the 1999 cost projections for planar anode supported SOFC stacks should still be achievable. In the present study, the net result of increases and decreases in factors influencing the cost resulted in approximately a 5% increase in cost of the baseline case to $90/kW. Increases in processing costs, primarily driven by the addition of QC steps, were greater than the reductions in material cost, primarily driven by lower assumed costs for YSZ. The lower power density of the 2003 baseline case further accentuated the increases on an kW basis. The anode and interconnect dominated the stack cost contributing approximately 90% of the cost. Quality control will be critical to successful assembly of stacks with high yields. If defective EEAs pass through final inspections prior to stack assembly at even a 1 percent level, stack cost could increase by more than a factor of 2 above the baseline projection. The stack yield will be influenced by the number of cells which can impact decision on stack voltage and stack interconnect costs for a targeted system voltage.

Achievement of high power densities will be important for low cost due to the large contribution (approximately 85% at high production volumes) of materials to the stack cost. The inclusion of a performance thermal mechanical model is important for analyses of this type because real kinetic data, ohmic losses, stack design parameters, mass transport limitations, and temperature gradients can be factored into the projected power density without violating utilization assumptions. Minimization of the thickness of the EEA layers will contribute to increased power density with the electrolyte being the most important factor. In our analysis, the temperature gradient across the stack was limited to 150^{o}C, however, stacks with a higher tolerance to thermal gradients could lead to higher power densities and lower costs.

Significant economies of scale are realized in going from a production volume of 5 MW to 250MW, with approximately 60% of the reduction realized in stepping up to 25 MW. For this analysis, reductions in process costs due to higher utilization of capital equipment were a major factor in the decrease in cost.

The SECA Team inputs were important in directing the project efforts to issues critical to SOFC technology development. Going forward, the Teams expressed strong interest estimating the cost and assessing the technology of balance-of-plant (BOP) components such as recuperators, air management systems, components for interconnecting large arrays of small stacks, and power electronics. Augmentation of the cost model with the performance model provided significant benefit for this analysis, but should provide even more valuable insights in the future as developers consider the tradeoffs between stack operating temperatures, material selection options, and BOP costs.

2. INTRODUCTION

2.1. SECA Program

The Solid State Energy Conversion Alliance (SECA) has defined a path to making fuel cells a reality involving technology and market development through a government – industry partnership. The SECA targets include:

- **2005** First generation products with specialty markets such as truck auxiliary power units (APU's), recreational vehicles (RV's), and military applications as early adopters
- **2010** Commercial products targeted to residential, commercial, and industrial combined heat and power, and transportation APU's markets. A factory manufacturing cost of $400/kW has been set as a goal.
- **2015** Larger scale power plants with higher efficiency (hybrid plants with 60-70%) and a manufactured cost of $400/kW.

The SECA industry teams include: Acumentrics, Delphi, Fuel Cell Energy, General Electric, Siemens-Westinghouse, and SOFCo, each pursuing individual technology paths (e.g., stack design – tubular versus planar anode supported, size – kilowatts to megawatts) and markets. In parallel with stack and balance-of-plant (BOP) technology developments, cost effective manufacturing processes and stack materials must be developed to achieve the SECA factory cost target of $400/kW.

Within SECA, the Core Technology Program (CTP) has the following main objectives:

- Generate new scientific and engineering knowledge to better enable SECA Industry Teams to develop low-cost solid-oxide fuel cell (SOFC) power generation systems.
- Create technology breakthroughs to address technical risks and barriers that currently limit achievement of the SECA performance and cost goals for SOFC systems.
- Transfer new science and technology developed in the Core Technology Program to the SECA Industry Teams.

The CTP consists of two phases:

- Phase I: a one-year effort to investigate and evaluate the feasibility of proposed solutions and/or the merits of a scientific path of inquiry,
- Phase II: to mature the science and technology developed to a sufficient level that it can be utilized by the SECA Industry Teams.

2.2. 1999 FETC SOFC Cost Analysis Overview

The National Energy Technology Laboratory (NETL) has a long history in high temperature fuel cell technology development. The assessment of manufacturing technologies and cost has been an integral component of these due to the criticality of both to the commercialization of fuel cells in a competitive market place. In 1999, TIAX [2] (as the Technology and Product Development sector of Arthur D. Little) conducted a technology and cost assessment of anode supported planar SOFC technology with metallic interconnects. The cost of this lower temperature SOFC technology (<800^{o}C) was compared to a high temperature (1000^{o}C) planar all ceramic design. For the low temperature planar technology with metallic interconnects, a manufacturing cost projection of \$430/m^2 was obtained through an activities-based cost model. For an assumed power density of 500 mW/cm^2 this translates into a cost of \$86/kW for materials and processing, significantly less than the all ceramic high temperature stack with a cost of \$377/kW. Several factors contributed to the lower overall stack cost:

- Lower temperature permitted the selection of a much less expensive interconnect material, ferritic stainless steel
- Anode support of the cell allows use of a thin electrolyte leading to higher power density and much less YSZ material.

The lower projected overall cost for low temperature SOFC technology increases the likelihood of commercial success of SOFCs. Several SECA teams, General Electric and Fuel Cell Energy, with their acquisitions of Allied Signal and Global Thermal Electric SOFC technology respectively, have entered the low temperature planar anode supported arena.

2.3. 2003 NETL SOFC Cost Analysis Project Objectives and Approach

2.3.1. Project Objectives

As part of the 2002 solicitation for the CTP, NETL sought proposals to develop analysis methods and computational codes for analyzing SOFC production process issues in order to aid development of optimal production process methods, rates, and controls. The 1999 cost assessment considered cost at a high level and did not get into the cost implications of practical manufacturing issues such as part flatness and residual stresses associated with different manufacturing processes and SOFC designs. NETL sought development of a model with the capability to:

- Handle all key SOFC stack components, including ceramic cells and interconnects
- Relate manufactured cost to product quality and likely performance, taking into account manufacturing tolerances, product yield, and line speed

- Address a range of manufacturing volumes ranging from tens to hundreds of megawatts per year
- Adapt to individual production processes under development by SECA industrial teams

The main objective of Phase I is to build a basic frame work that will be used for modeling and planned manufacturing processes of the current SECA industrial teams, and demonstrate the framework with a relevant example process in detail.

2.3.2. Project Approach and Deliverables

The proposed project approach consisted of two phases as summarized in Figure 1. In Phase I, of this project, the emphasis was on demonstration of the capabilities of the cost model to the SECA Industry teams and getting their inputs on critical issues. Figure 2 breaks out the proposed Phase I effort into three tasks, however, after discussions with the SECA teams, they preferred the use individual meetings with each team rather than collective workshops as a means of collecting information. In addition, the teams did not want to access the cost model through an internet-based-user interface. For Phase I, only non-proprietary discussions were held and the cost model demonstration was conducted using generic information in the public domain. Several of the SECA teams provided inputs on topics of interest for this analysis and feedback on the draft final presentation. After the initial face-to-face meetings, subsequent discussions were conducted at SECA meetings or over the phone.

In addition to updating the results and assumptions of the 1999 project, the cost model was augmented with a SOFC performance model to calculate power density, utilization, temperature gradients, and mechanical stresses in the stack, the latter during steady state operation and thermal cycling. Addition of this capability permits one to evaluate the impact of improvements in electrochemical performance, changes in power density as the stack design changes (e.g., thickness of individual layers, changes in active area and flow field design), and changes in material properties. The model was also used to calculate maximum stresses on the materials and after comparison with failure cures to estimate mechanical failures due to cracking. In contrast, the 1999 model simply selected an average power density and assumed that the utilization could be achieved and the materials would survive any stresses arising from thermal gradients.

In addition to the deliverables identified in the figures, the manufacturing process analysis was assessed to identify critical manufacturing steps and performance parameters. If considerable uncertainty exists about these steps, specific additional SECA R&D objectives might have been developed. Cost modeling in concert with practical pilot line experience can identify manufacturing issues with significant economic impact.

	Phase I SOFC Manufacturing Model Framework and Demonstration	Phase 2 SOFC Manufacturing Model Expansion and Use
Objectives	◆ Develop model framework ◆ Demonstrate benefit of model for system development trade-off analyses ◆ Develop Phase 2 plan	◆ Expand Phase I model framework to other SOFC system designs, alternative materials, and manufacturing processes ◆ Incorporate findings and research of SECA teams
Deliverables	◆ Model framework ◆ Demonstration of model capabilities	◆ Workshop with SECA stakeholders

Figure 1 Project Overview

	Task 1 Model Framework Development	Task 2 Model Demonstration	Task 3 Reporting
Objectives	• Develop architecture of manufacturing model • Review architecture with SECA stakeholders	• Revise existing model architecture based on Task 1 workshop • Demonstrate manufacturing model with baseline SOFC system	• Report project progress • Prepare Phase I report that summarizes critical manufacturing steps and performance parameters • Define Phase II development effort
Deliverables	• Workshop with SECA stakeholders • Definition of model framework, user interface with model, and critical issues to be assessed, model assumptions	• Workshop with SECA stakeholders	• Monthly updates • Phase I final report

Figure 2 Description of Phase I Year 1 Tasks

2.3.3. Cost Model Benefits to the SECA Industrial Teams

The benefits of the model users are as the following:

- The model will allow developers, and NETL to minimize the uncertainties inherently associated with commercialization of a new technology.
- The model is structured to facilitate the development of versions for the specific stack designs and manufacturing processes that the industrial teams are considering.
- The model will handle all key SOFC stack components, including ceramic cells and interconnects.
- The product quality and likely performance are taken into account to manufacturing cost, such as product yield, line speed, etc.
- Sensitivity analysis and Monte Carlo simulation will allow users to identify the main cost driver in their manufacturing cost system.
- Scenario analysis will help user balance the trade-off in different product design, material selection, and process flow, etc.
- The production volume scaling is ranging from tens of MW to hundreds of MW per year.

2.3.4. SECA Team Feedback

To demonstrate the capabilities of the integrated cost and performance models the Teams expressed interested in an assessment of the impact of layer thickness on cost and performance. In the absence of mechanical considerations, reduction of layer thickness should increase power density due to reduced ohmic losses, however, concerns were expressed that the mechanical robustness would be degraded leading to cracking and yield losses. The integrated model can not account for changes in barrier properties of the electrolyte due to defects or increased diffusion through a thinner layer and the consequences, lower efficiency due to decreased utilization and increased cathode polarization.

The Teams also expressed an interest in a more detailed accounting of Quality Control costs in the process. In the 1999 study, a final pressure test for pinholes in the completed electrode electrolyte assembly (EEA) was included in the process, however, provision was not made for upstream inspections. Through discussions with Oak Ridge National Laboratory (ORNL)[i], several inspections technologies under their consideration were incorporated into the process flow along with their relationships for the probability of material failure versus stress. The report describes these methods in more detail along with equipment costs obtained from suppliers. Different QC strategies were considered and their impact on final yield assessed. In addition to assessing the impact of EEA yield on cost, the impact of defective EEAs on stack yield was also considered.

Sealing of stacks is a critical challenge for developers of planar SOFCs. Without inputs from developers on reasonable seals designs and manifolding, the decision was made to exclude sealing materials and associated production processes from the cost model. Consequently the costs of seals, manifolds, and other packaging materials (e.g., insulation) should be added to the

[i] Discussions with Edgar Lara-Curzio, ORNL

cost values generated in this analysis. The Teams confirmed that we should be considering both co-fired and multi-fired process flows.

The following report discusses the results in greater detail. Detailed information on process assumptions has been placed in the Appendix. As with any model, presentation of the assumptions is critical to the reader’s ability to understand the conclusions and to extrapolate the results to their own circumstances.

3. 1999 Cost Results

3.1. 1999 Cost Model Assumption

3.1.1. *Stack Description*

An anode supported planar SOFC stack with metallic interconnects was used as the basis for developing the bill-of-materials and manufacturing process for this analysis. Figure 3 illustrates a baseline planar SOFC repeat unit structure. Table 1 lists the thickness and material assumed for each layer of the baseline repeat unit along with estimated weights and volumes. Overall, the stack design used had a density of 3.2 g/cm^3 and a pitch of 5 cells per inch.

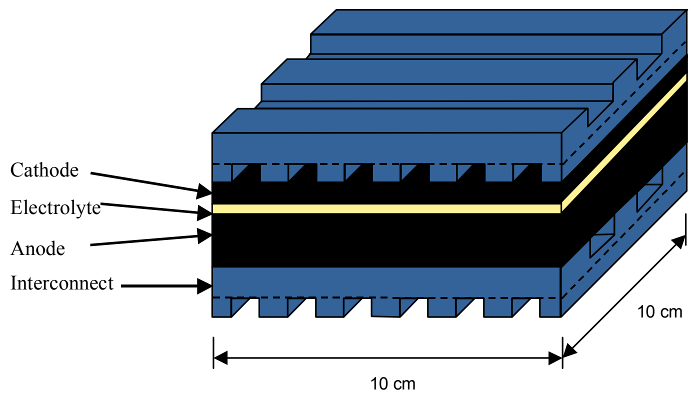

Figure 3 Schematic Baseline Planar SOFC Repeat Unit Structure

		Material	Thickness (µm)	Wt./area (g/cm^2)	Vol./area (cm^3/cm^2)
Electrochemical Layers	**Anode (µm)**	Ni-cermet	700	0.36	0.08
	Electrolyte (µm)	8 YSZ	10		
	Cathode (µm)	LSM	50		
Interconnect		SS430	4320	1.29	0.43
Total Cell	Pitch: 5 cells/in Density: 3.2 g/cm^3			1.65	0.51

Table 1 1999 Stack Description

3.1.1.1. SOFC Components

Cathode: The cathode is a porous layer that facilitates the transport of oxygen to the reaction zone (electrolyte / cathode interface) and conducts the electrons and heat from the reaction zone. The doped $La_{1-x}Sr_xMnO_{3-\delta}$ (Lanthanum strontium manganite (LSM), 0.15 < x < 0.25) is the commonly used cathode material and is mixed with YSZ (e.g., YSZ/LSM – 1:1) to increase the 3-phase electrochemical interface (O_2/LSM/YSZ)

Electrolyte: The common electrolyte is yttria stabilized zirconia (YSZ) in a dense gas barrier layer with O^{2-} ion conductivity.

Anode: The anode is a porous layer that facilitates transport of hydrogen and reformate to the reaction zone and conducts the electrons and heat from the reaction zone. The anode must be a good electronic conductor to transfer the electrons to interconnect. It also needs high porosity to transfer hydrogen gas through anode to the electrolyte and remove the product water. The typical nickel cermet anode is prepared from a 1:1 weight ratio mixture of nickel oxide and YSZ. Anode porosity is about 25 to 40 volume percent [5].

Interconnect: The interconnect is an electrically conductive barrier layer that connects unit cells in series in the stack. It isolates the anode and cathode reactant streams, distributes the reactant gases to the electrodes, and distributes heat. The choice of interconnect material (metallic or ceramic) depends on the operating temperature. In high temperature systems, e.g. 900-1000^{o}C, lanathanum chromite and high chrome alloys has been used as the interconnect, while ferritic stainless steels are being used at temperatures less than 800^{o}C. Coatings are generally used with the metallic interconnects to prevent oxidation on the cathode side. In addition to oxidation properties, the coefficient-of-thermal expansion of the interconnect must be matched to the electrode electrolyte assembly.

3.1.2. Process Assumptions

Both multi-fired and co-fired process flows (shown in Figure 4 and Figure 5) were evaluated in this analysis. The co-fired process offers the potential of eliminating a sintering step but does not allow tailoring of sinter temperatures for each layer.

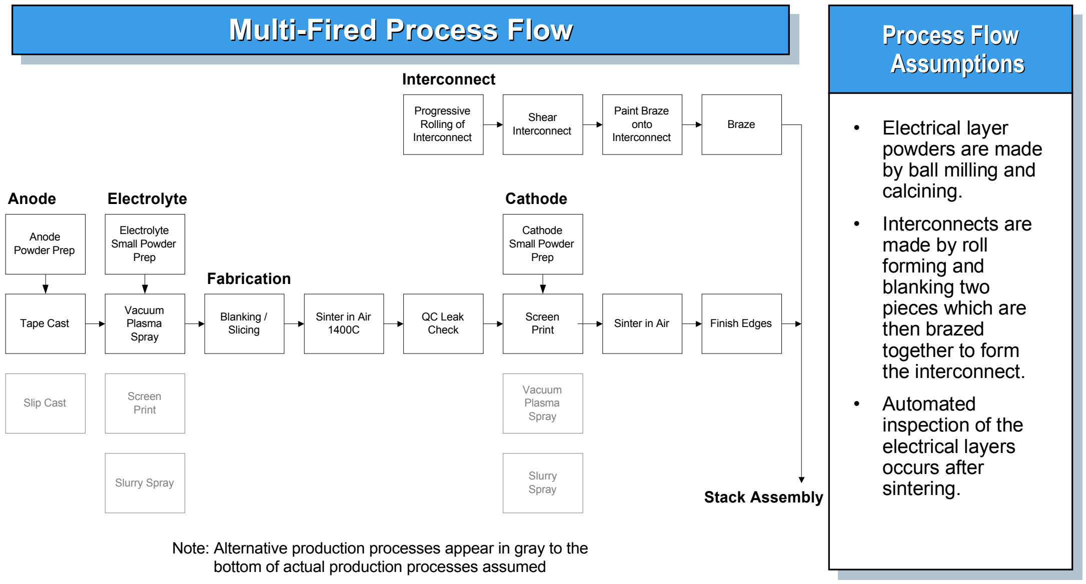

Figure 4 1999 Manufacturing Cost Model Multi-Fired Process Flow

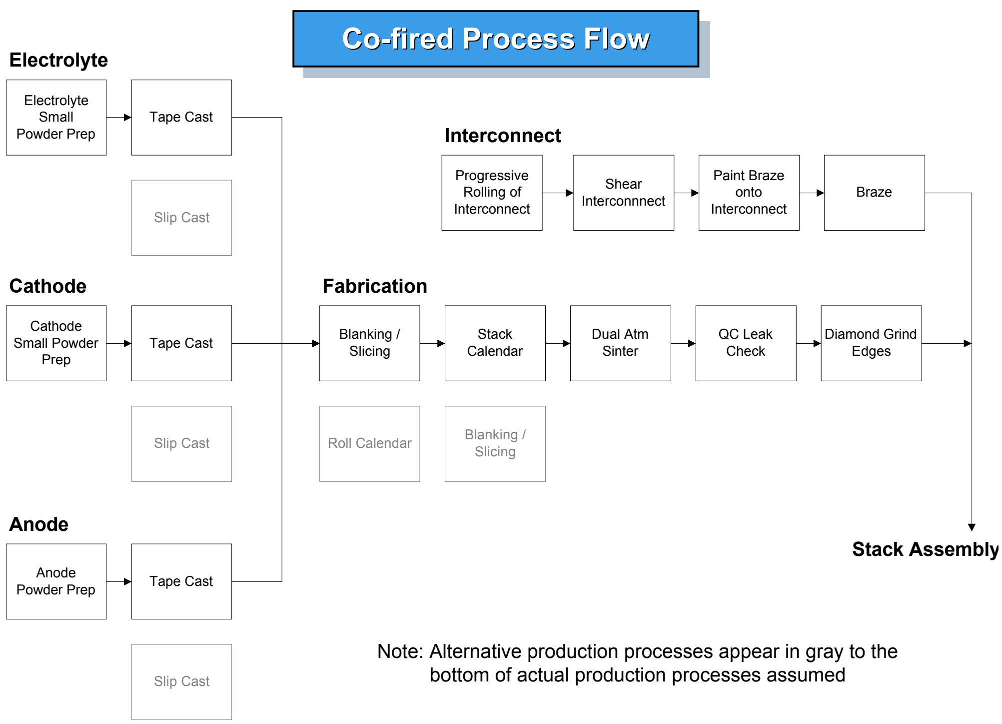

Figure 5 1999 Manufacturing Cost Model Co-Fired Process Flow

3.2. 1999 Manufacturing Cost Model Results

In this study, the cost of the multi-fire process was found to be approximately 10% higher than the co-fired process. However, the multi-fired process may be technically more attractive because sintering conditions can be tailored to the individual layers. In both processes, materials were the major contributor (representing 70 – 75%) of the factory cost representing 70-75%.

Baseline Assumptions: 5 cells/inch, 500 mW/cm^2, 250 MW/year

Multi-Fire

		$/kW Mat	$/kW Process
Process Flow Steps	Anode	$40.83	$1.63
	Cathode	$0.90	$0.50
	Electrolyte	$7.14	$0.60
	Interconnect	$16.39	$3.42
	Layer Assy		$18.75
Sub-Total		$65.26	$24.91
Total		**$90.18**	

Co-Fire

		$/kW Mat	$/kW Process
Process Flow Steps	Anode	$39.22	$2.51
	Cathode	$1.08	$1.49
	Electrolyte	$2.53	$1.23
	Interconnect	$16.39	$3.42
	Layer Assy		$12.11
Sub-Total		$59.22	$20.75
Total		**$79.97**	

Table 2 1999 Manufacturing Cost Breakdown on $/kW Basis

The anode and interconnect layers dominated the total unit cell costs for both the co-fired and multi-fired processes.

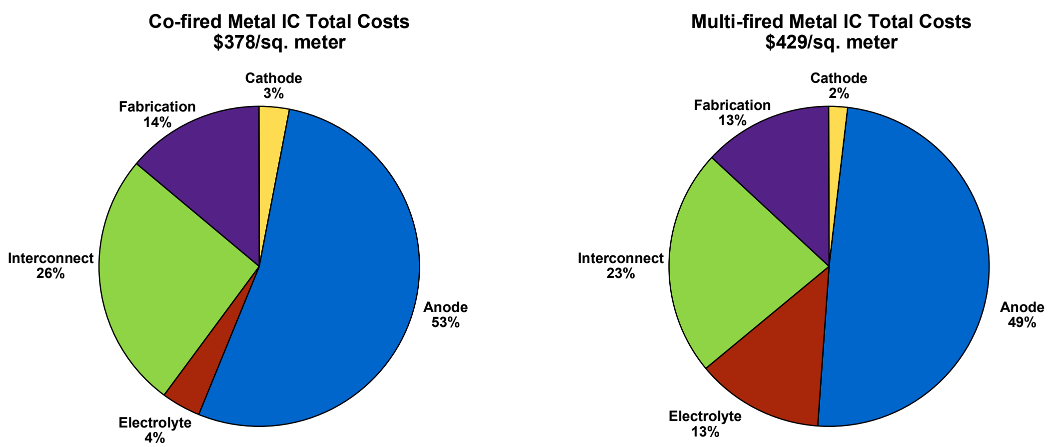

Figure 6 1999 Manufacturing Cost Break Down on an Area Basis

4. MODELING METHODOLOGY

4.1. Performance/Thermal/Mechanical Model Approach

4.1.1. Background

A set of finite element-based models for simulating the electrochemical performance and estimating the thermo-mechanical stresses of SOFCs was developed under previously funded DOE and NETL programs[ii]. For this project we improved these models to take into account variable electrode and electrolyte layer thicknesses, operation on pre-reformed fuel, and appropriate mechanical and thermal boundary conditions for the particular stack design being considered. The performance model was then used to generate a functional form for the predicted average power output in terms of individual layer thickness values. The structural model was used to determine peak tensile stress levels in the ceramic EEA during manufacturing and subsequent operation. By combining these results with intrinsic statistical failure properties for the individual materials, expected manufacturing yield levels were calculated as functions of the cell geometry. The determinations of power output and material yield were incorporated directly into the manufacturing cost model so that their effects on total cost and cost-per-kilowatt were automatically included in the results.

4.1.2. Methodology

The performance model was developed for a planar ceramic EEA sandwiched between ferritic stainless steel interconnects, representative of a cell in a stack (see Figure 7). The analysis was performed using the transient thermal analysis capabilities of the ABAQUS commercial finite element package, with custom subroutines that we created to capture the electrochemical reactions, multi-component species diffusion, and water-gas shift reaction in the fuel channels. Figure 8 illustrates the breakdown of the model and Table 3 highlights the key assumptions, primary uses, and outputs from the model. The model described here only included hydrogen oxidation, which sufficed for gaining a perspective on the stress distribution in cells during operation. Other fuels, shift reactions, and internal reforming can be easily added.

[ii] See "Structural limitations in the scale-up of anode supported SOFCs," Final Report delivered to DOE under contract 736222-3003 (2002).

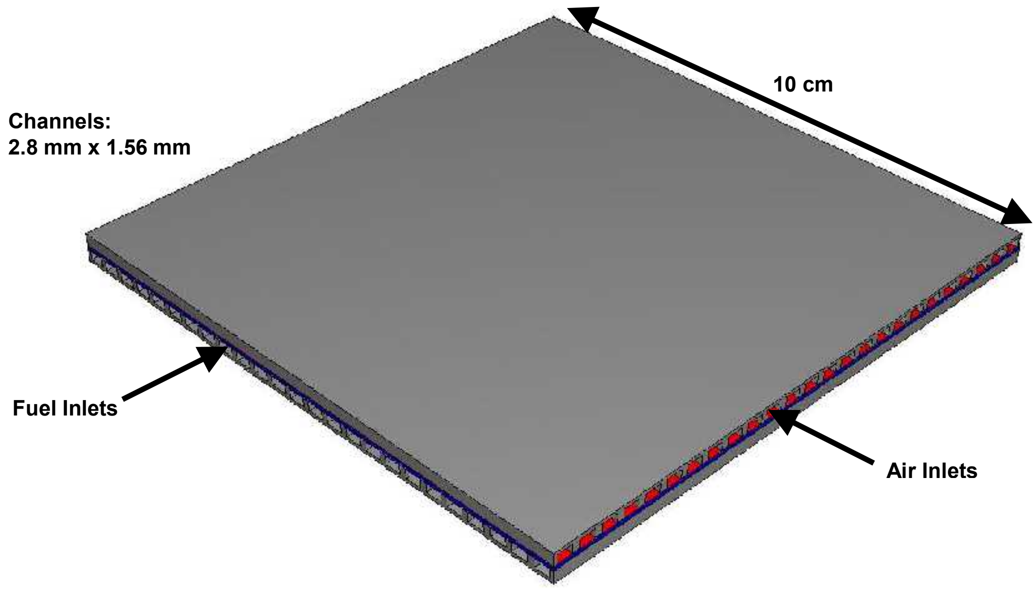

Figure 7 Typical Geometry of Finite Element Simulations for Performance Modeling

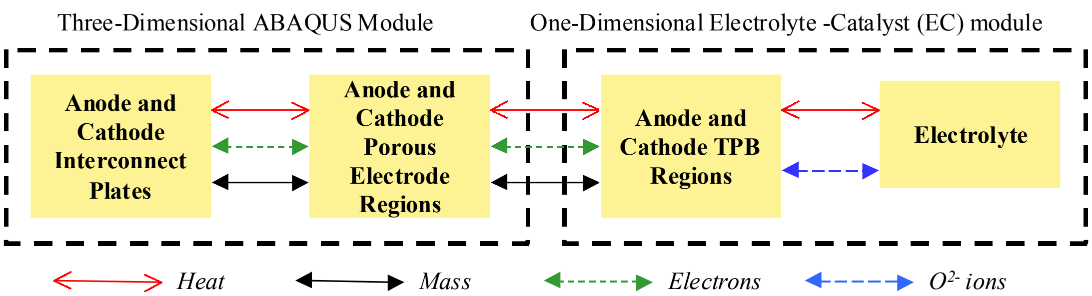

Figure 8 Model Structure

Cell Configurations simulated	Key Assumptions	Output	Primary uses
• Small and large area anode supported SOFCs with metallic interconnects • High fuel utilization, non-isothermal operation • Steady state and transient operation, including stack start-up and shut-down	• Adiabatic or steady heat loss from outer edges • Plug flow in flow channels • 2-d diffusion in porous electrodes • Reaction only in the reaction zone	• Spatial distribution of temperature, current density, stress, species concentrations, and overpotentials	• Understand effects of operating conditions and cell design on performance: Identify hot spots, regions of low current, high stress and potential failure mechanisms • Answer 'what-if' questions, such as effect of changes in operating conditions, dimensions, etc.

Table 3 Key Model Assumptions, Primary Uses, and Outputs

For a given set of operating conditions and cell design parameters, the time-dependent electrochemical reaction rates were estimated as a function of position within the cell. From this the average power density for the cell was computed. In addition, the steady-state temperature distribution generated by the heat release in the fuel channel and at the electrode/electrolyte interface was captured for subsequent thermo-mechanical analysis.

Base Case Assumptions

The following were the conditions and cell design parameters assumed for the base case simulations:

Operating conditions:

Cell voltage: 0.7 V

Reactants inlet temperature: 650°C, which is consistent with our system level analysis[iii]

Fuel: Reformed natural gas composed of 74.6% H_2, 3.9% CH_4, 11.5% CO, 10.0% CO_2

Fuel utilization: 85 %

Oxidant: Air

Maximum cell temperature: 800°C

Air stoichiometry: Adjusted to maintain the cell temperature below 800°C

Design parameters:

Anode thickness: 700 μm

Electrolyte thickness: 10 μm

Cathode thickness: 50 μm

Flow configuration: Both co-flow and cross-flow cases were simulated. However, as shown below, the power density estimates were almost identical for the two cases. Also, since the co-flow simulations converge more rapidly than the cross-flow simulations, the majority of the calculations were performed with the co-flow configuration.

Contact resistance: A uniform contact resistance of 0.1 ohm/cm^2 was assumed.

The stress model consisted of the simulation of the anticipated processing steps used to create the EEA, assembly into the stack, and subsequent operation at steady state. The in-plane stresses that arise due to thermal expansion mismatch among the anode, electrolyte, and cathode were derived using literature values for the elastic and thermal properties of each layer material. Two processing scenarios were modeled: co-sintering of the three layers at 1400^{o}C; and a two-stage process involving the firing of the anode and electrolyte together at 1400^{o}C, followed by deposition of the cathode and firing of the assembly at 1050^{o}C. With the EEA in its residual stress condition at room temperature, the assembly into a stack was simulated using the quasi-static stress analysis capabilities of ABAQUS. Contact between the electrodes and the ribs of the interconnects was specified, and an out-of-plane pressure load was applied corresponding to the typical clamping force required for sealing in a stack (approximately 440 kPa). Starting from this clamped configuration, the steady-state temperature profile obtained from the performance

[iii] See "Conceptual design of POX / SOFC 5 kW net system," Final Report submitted to DOE under contract 73622-3002 (2001)

model was applied to the EEA and interconnects, and the resulting thermo-mechanical stress state was determined.

Since the probable failure mode of the ceramic materials is by crack initiation and propagation, the predicted peak tensile stress experienced throughout the processing steps was recorded for each layer. This peak stress level was then used in combination with Weibull statistical models for brittle fracture to obtain an expected material failure probability. The failure models were based on fracture experiments performed on SOFC materials by Edgar Lara-Curzio at ORNL. For a given stress level σ, the cumulative probability of failure is given by

$$F(\sigma) = 1 - \exp[-(\sigma/\eta)^{\beta}],$$

with the parameters for each material given in Table 4. The resulting probability curves are depicted on a log-log scale in Figure 9.

Layer	η	β
Cathode (YSZ - LSM)*	105.9	3.5
Electrolyte (YSZ)	216.3	2.6
Anode (Ni - YSZ)	105.9	3.5

* Insufficient data on the strength characteristics of YSZ-LSM were available. Because of the similarity of the materials, experimental results for Ni-YSZ were used for both anode and cathode.

Table 4 Weibull Parameters for SOFC Material Failure Statistics (Data from ORNL)

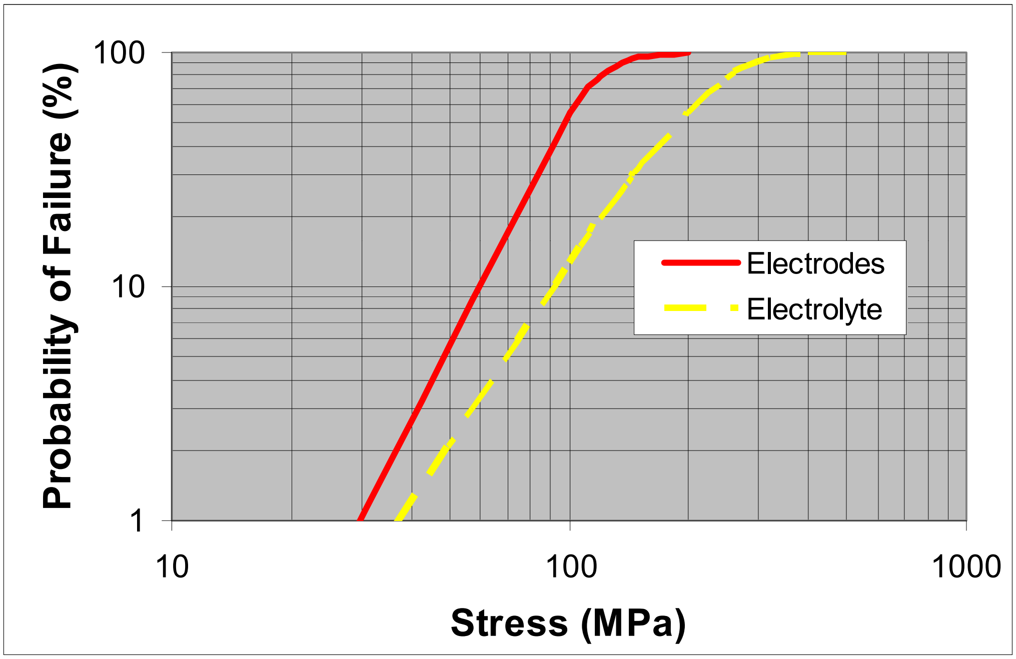

Figure 9 Failure Probability Curves as a Function of Peak Tensile Stress (Data from ORNL)

The results of the performance and structural models, as well as the material failure statistics, were expressed in functional form to capture the dependencies on individual EEA layer thicknesses. These functional forms were then integrated into the overall cost model to enable automatic projections of the interactions among power density, stress, material yield, and cost.

4.2. Manufacturing Cost Model Description

The model provides SOFC manufacturing costs based on changes in variable inputs to the SOFC design parameters (system design-performance module), material selection (materials database) and manufacturing processes (process database). The boundary conditions and primary relationships for system design parameters, material specifications and manufacturing process flow are integrated into the model architecture. Cost outputs from the model are categorized by materials, labor, utilities, equipment, tooling, building, overhead labor, maintenance, and the cost of capital.

The model development followed a logical flow that invites participation of all stakeholders (DOE, industrial teams, national labs, other SECA participants) at regular intervals. The cost model is constructed using TIAX proven technology-based cost modeling methodologies and build off our previous model developments and experience with the development of SOFC costing programs. In this study, the cost model focused on key SOFC stack components, including the ceramic layers and metallic interconnect. The seals, manifolds, and balance of plant (BOP) were not considered for this demonstration.

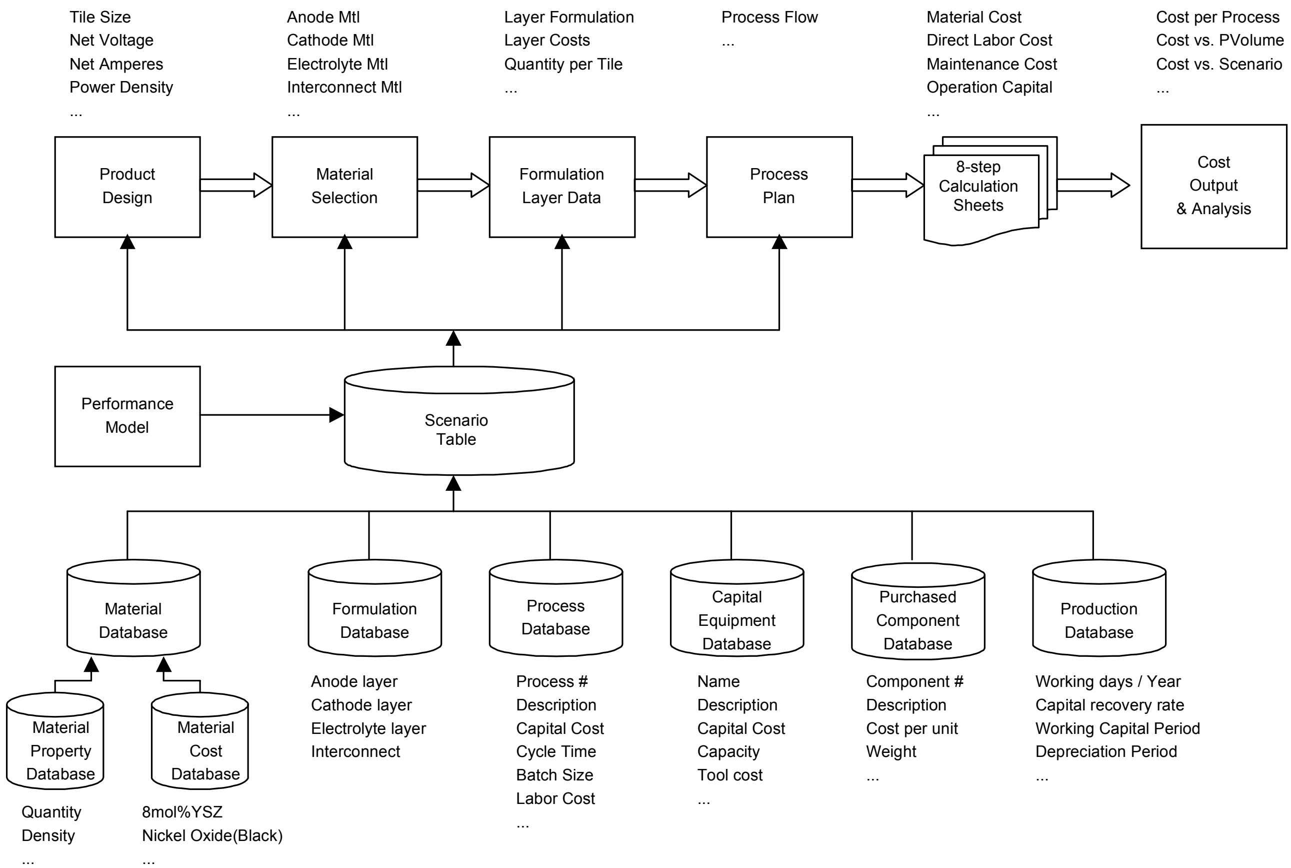

Figure 10 Manufacturing Cost Model Schematic

4.2.1. Cost Definition

For this study, the manufacturing cost model focused on factory cost, which includes direct labor, direct materials and factory expense. The R&D, factory overhead, and general expense costs are not included. Figure 11 shows the items included and excluded in the reported factory cost.

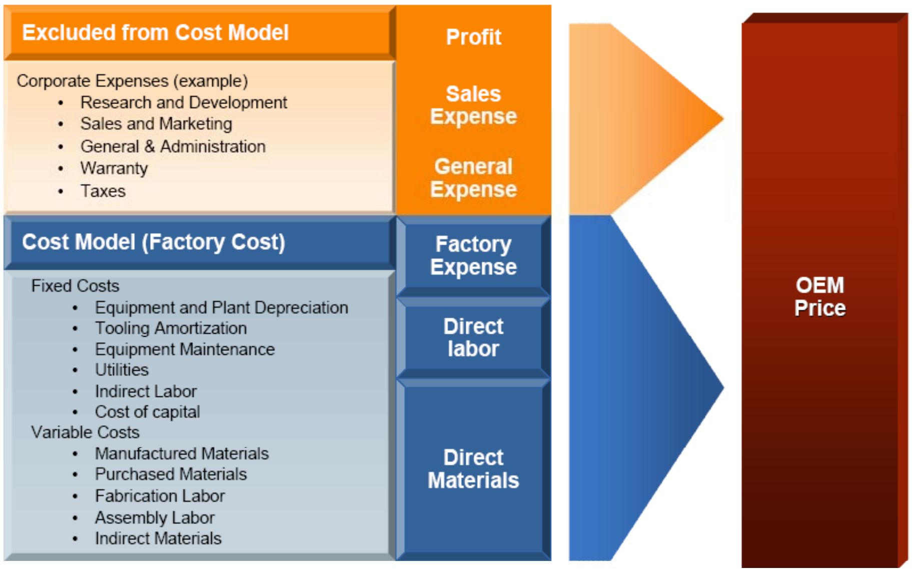

Figure 11 Costs Structure

4.2.2. Cost Modeling Methodology

A five-step approach for conducting manufacturing cost analysis was used.

Step 1. Product and manufacturing process definition: Identification of detailed product design parameters and manufacturing process options. Key elements are material type and quantity, process cycle time, production equipment specifications, and direct labor requirements.

Step 2. Production process scenario definition: The production process scenario is critical for identifying realistic and credible manufacturing costs based on current manufacturing process capabilities. Key elements include annual production volumes, plant size and location, internal and out-source operations, and wage rates.

Step 3. Development of a cost model with defined product and manufacturing processes: A cost model is constructed that provides product/process costs based on variable inputs. Cost outputs from the model are categorized by materials, labor, utilities, equipment, tooling, building, overhead labor, maintenance, and cost of capital. The structure of the model permits frequent and complex analyses of multiple input.

Step 4. Development of cost models for relevant competitive design options and manufacturing processes: In order to make cost comparisons of competing technologies, design options, and alternative manufacturing processes, additional models/scenarios derived from the initial customized model are developed. The structure and consistent approach of our manufacturing cost model permits accurate and rapid comparisons.

Step 5. Sensitivity, Scenarios, Economic scale analysis and Monte Carlo simulation: These analysis provide an in-depth understanding of the key cost drivers in each technology and design option, the critical manufacturing processes for cost reduction initiatives, and the economic risks associated with selected development and commercialization strategies.

4.2.3. Databases

Figure 12 illustrates the material, process, purchased component, and production databases for the manufacturing cost model. Users input the data based on the product design and production volume. The data can come from vendor quotes and discussions, as well as TIAX industrial experience.

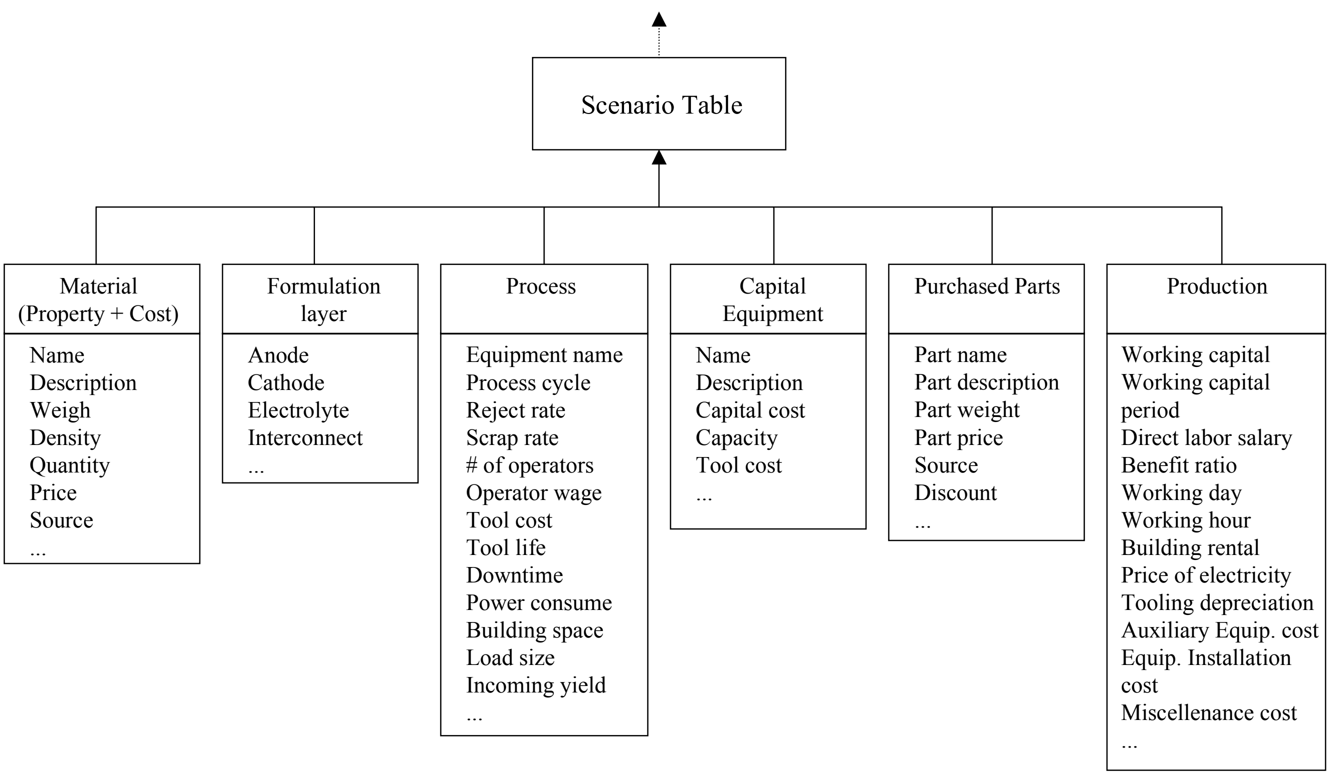

Figure 12 Manufacturing Cost Model Database Diagram

4.2.4. Process Flow

Process planning is one of the most important parts of the manufacturing cost model. The processes are divided into six categories, e.g., Anode, Electrolyte, Cathode, Interconnect, Layer

Assembly, and Stack Assembly. Users can fill in the process flow by selecting the suitable processes in the process database. For example, to make the cathode layer, a user can pick ball milling I, ball milling II, de-aeration and tape casting as a possible scenario. Figure 13 illustrates the simplified co-fired process flow for the stack.

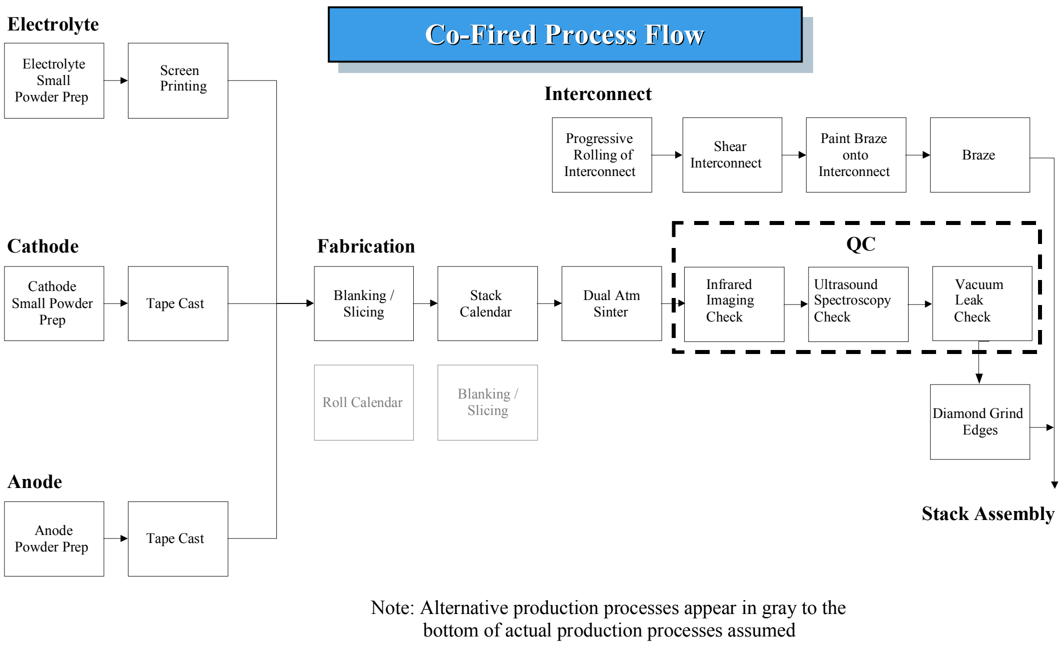

Figure 13 Co-Fired Process Flow

4.2.5. Materials

The anode and cathode tape casting formulations are shown Table 5 and Table 6.

Anode Materials	Weight Percentage
Nickel 255	47%
Nickel Oxide (black)	13%
Titanium Dioxide	1%
TZ8Y- Yttria	11%
Cerium Oxide	1%
Binders	
Butvar B98	1%
2-Propanol	9%
2-Butoxyethanol	17%

Table 5 Anode Layer Materials and Binders

Cathode Materials	Weight Percentage
LSM	53%
Binders	
Methocel	30%
2-Butoxyethanol	17%

Table 6 Cathode Layer Materials and Binders

The screen printing formulation for the electrolyte is shown in Table 7.

Electrolyte Material	Weight Percentage
8 YSZ	70%
Binders	
Santicizer 160	6%
Butvar B76	6%
n-Butylacetate	18%

Table 7 Electrolyte Layer Material and Binders

For this study, the interconnect is fabricated from ferritic stainless steel 430 sheet.

4.2.5.1. Material Calculation

Material cost contains two contributions, the design product material and the material lost in process due to scrap and yield losses. Yield losses arise from defective parts, while scrap arises from incomplete utilization of materials, e.g., material not used after die-cutting parts from a sheet. From the repeat unit dimensions, density, and layer formulation, we can calculate the design product material cost assuming no scrap and yield losses.

Figure 14 shows how the design product material cost is calculated.

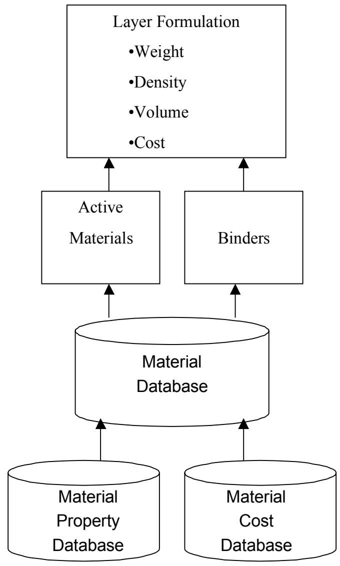

Figure 14 Design Product Material Calculation Flow

4.2.5.2. Material and Process Cost Calculation

For this study, a spreadsheet was constructed with multiple columns set up for each process step. Table 8 illustrates the basic data structure for one process step. The manufacturing cost includes three categories, variable cost elements, operation fixed costs, and non-operation fixed costs. Variable costs include the material cost, direct labor cost, and utility cost. Operation fixed costs include the tooling cost, maintenance cost, indirect labor cost, and operational capital cost. Non-operation fixed costs include the equipment cost, building cost, and non-operational capital cost.

PROCESS OPERATION: FoilAn- Weigh Powders
© TIAX LLC

OPERATION COST SUMMARY	per piece	per year	percent	investment
VARIABLE COST ELEMENTS				
Material Cost	$1.4814	$6,073,727	97.3%	
Material Scrap Credit	$0.0000	$0	0.0%	
Direct Labor Cost	$0.0003	$1,113	0.0%	
Utility Cost	$0.0000	$57	0.0%	
OPERATING FIXED COSTS				
Tooling & Fixtures Cost	$0.0000	$0	0.0%	$0
Maintenance Cost	$0.0007	$3,048	0.0%	
Indirect Labor Cost	$0.0001	$286	0.0%	
Cost of Operating Capital	$0.0372	$152,585	2.4%	
OPERATING VALUE ADDED	$1.5197	$6,230,816	99.8%	$0
NON-OPERATING FIXED COSTS				
Equipment Cost	$0.0004	$1,620	0.0%	$16,200
Building Cost	$0.0007	$3,000	0.0%	$60,000
Cost of Non-Operating Capital	$0.0020	$7,997	0.1%	
TOTAL VALUE ADDED	$1.5228	$6,243,433	100.0%	$76,200

Table 8 Sample Cost Model Calculations Sheet

The total manufacturing cost is then calculated by summing the individual process steps. Total cost is reported on an area basis ($/m^2) and on a power ($/kW) basis according to the stack power density.

4.3. Quality Control

We have incorporated additional non-destructive inspection steps based on discussions with ORNL to better capture costs associated with quality control. Infrared imaging and ultrasonic spectroscopy were added to the inspection processes. Figure 15 illustrates how these three inspection steps are used to capture different types of defects and to cost effectively reject defective EEAs. See detailed descriptions in appendix.

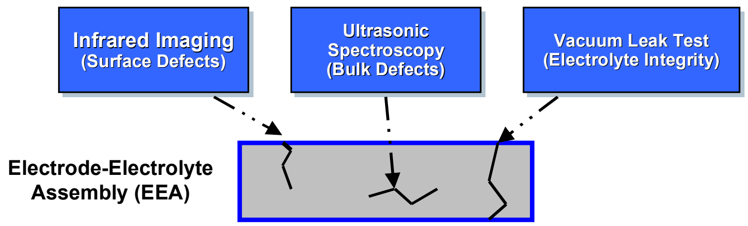

Screen	First	Second	Third
Method	Infrared Imaging	Ultrasonic Spectroscopy	Vacuum Leak
Type of Defect	Surface	Surface and Bulk (Orientation Dependence)	Through (leaks)
Through put	High	High	High
Cost	Medium	Low	High

Figure 15 Three EEA's Inspection Processes

When stack fabrication moves from the laboratory to the pilot plant and then to the full scale manufacturing plant, quality control will become very important to the final stack cost. The following QC analyses were integrated into manufacturing cost model:

- Inspection accuracy level
- Yield vs EEA defective rate
- Stack cost vs EEA defective rate

4.3.1. Inspection Accuracy Level

Figure 16 illustrates a sample manufacturing process flow. By varying the quality inspection accuracy in steps QC-1 and QC-2 steps, the manufacturing cost model will compute and compare the final stack costs.

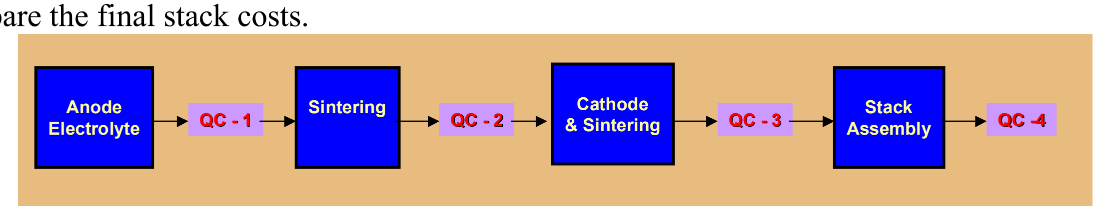

Figure 16 Quality Control Process Sequence

Two QC scenarios were considered to illustrate the impact of different inspection test plans on the multi-fired process costs as shown in Table 9.

- Both scenarios catch all defective parts at QC-3 so that stacks can be assembled
- Overall line yield of 75% for Scenario I and II
- 100% accuracy for inspection

Scenarios	QC-1	QC-2	QC-3	QC-4
I	100%	100%	100%	100%
II	0	0	100%	100%

Table 9 Scenarios I & II

4.3.2. Yield vs. EEA Defective Rate

In the 1999 study, it was assumed that only good EEAs proceeded to stack assembly. In reality, some finite level of defective parts will escape detection and be built into stacks. The following equation shows the relation between stack defective rate and defective EEA rate. The number of EEAs in the stack, *n*, also affects the number of defects. . Normally, the higher the stack voltage (more EEAs in a stack), the stack defective rate becomes more sensitive to the EEA defective rate.

$$f_{Stack} = 1 - (1 - f_{EEA})^n$$

$$f_{Stack} : Stack\ \ defeactive\ rate$$
$$f_{EEA} : Defective\ EEAs\ rate$$
$$n : Number\ of\ \ EEAs\ in\ stack$$

Figure 17 shows the relationship between stack and EEA defects.

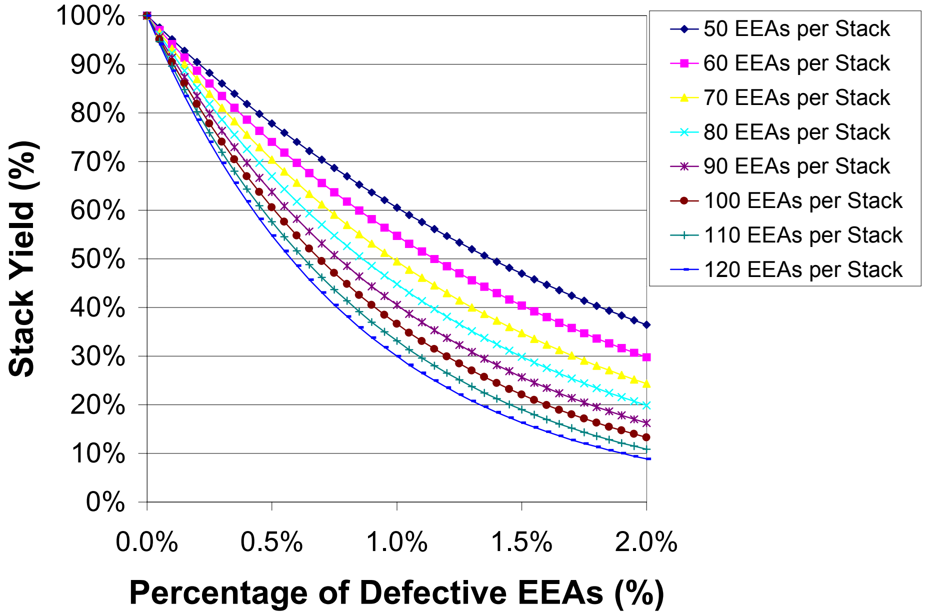

Figure 17 Quality Control Process Sequent

4.4. Economies of Scale

4.4.1. Objective

Current fuel cell manufacturing capacity is mainly laboratory based or at low pilot plant volume, but most cost studies focus on high production volumes. The objective of this analysis is to show the main cost drivers at different production volumes and to study the impact of production volume on process cost and material cost.

4.4.2. Methodology

Our baseline cost high volume study was conducted with an annual production volume of 250 MW. In this study, we assume that the annual production volume rises from 5 MW to 250 MW, correspondingly to 1,000 - 50,000 5 kW stack units annually.

To demonstrate the model capability, we primarily focused on the process and material cost analysis at different production volumes in calculating the scale-up stack cost. The process parameters and material costs are based on the conversations with industry contacts and our previous experience.

4.4.2.1. Process scale-up

To simplify the process options for this analysis, we divided the production level into three stages: manual, semi-automatic, and automatic. In each stage, all scenarios have the same process flow and equipment, even though the different scenarios have different production volume. For example, the 5 MW scenario and 25 MW scenario use the same process flow and type of equipment.

- Manual operation: The manual operation is for production volumes from 5MW to 25 MW, which uses manual equipment and has longer cycle times and smaller batch size. The equipment is designed for 25 MW or lower production.
- Semi-automatic operation: The semi-automatic operation is for production volumes from 25 MW to 150 MW, which uses medium size equipment and has partial automation in key stations. . The equipment is designed for 150 MW or lower production.
- Automatic operation: The fully automated operation is for high volume production from 150 MW to 250 MW. The workstations and material handling system are automated. The equipment is designed for 250 MW or lower production.

Table 10 lists the number of stacks and level of automation for the different production volumes.

Production Volume (MW)	# of Stacks (5kW)	Automation Level
5	1,000	Manual
25	5,000	
50	10,000	Semi-automation
100	20,000	
150	30,000	
200	40,000	Full automation
250	50,000	

Table 10 Manufacturing Process Scale-Up by Volume

4.4.2.2. Material Scale-Up

Material cost will also depend on the annual production volume. The anode material cost is approximately 50% of total material cost in our baseline model. The anode layer includes YSZ, Nickel 255, and Nickel oxide (black). The cathode layer is mainly LSM, but the quantity is very small and it is not major cost driver. The nickel and stainless materials are already mature high volume items and were assigned a smaller decrease in cost with volume than YSZ.

Econ. Volume (MW)	# of Stacks (5kW)	Nickel 255 ($/kg)	Actual Material Weight (kg)	Nickel Oxide ($/kg)	Actual Material Weight (kg)	8 mol% YSZ ($/kg)	Actual Material Weight (kg)	SS430 ($/kg)	Actual Material Weight (kg)
5	1000	$16.80	1284	$12.00	355	$100.00	335	$3.44	551
25	5000	$16.10	6421	$11.50	1776	$90.00	1675	$3.30	2753
50	10000	$16.10	12842	$11.50	3552	$80.00	3350	$3.30	5505
100	20000	$15.40	25683	$11.00	7104	$70.00	6700	$3.16	11010
150	30000	$14.70	38525	$10.50	10656	$65.00	10050	$3.01	16515
200	40000	$14.70	51366	$10.50	14208	$60.00	13399	$3.01	22020
250	50000	$14.00	64208	$10.00	17760	$55.00	16749	$2.87	27525

Table 11 Material Cost Scaled Up by Volume

- 8Mol% YSZ
  TIAX contacted major industry YSZ suppliers and found that YSZ price is most likely to be $40~$60/kg at annual order quantities of 10-20 metric tons. YSZ price might drop to $25 /kg at the annual order quantity of 60 metric ton. For the orders under 500kg, $100 /kg is a likely price. These are only rough projections and actual prices will depend on particle size, purity, and particle surface area. The prices might vary according to the particle size, purity, etc.

- Nickel 255 and Nickel oxide
  Nickel prices have been steady at $5-$8/kg. Nickel 255 and Nickel oxide price are quite steady even at different volumes.

- Interconnect
  We assume that interconnect is made from stainless steel 430 sheet. The price of SS430 sheet varies within 20% between low volume and high volume.

The following additional assumptions were made for calculating the effect of scale-up on the production cost:

- Multi-Fired process
  The multi-fired process was used for all scale-up scenarios. From the baseline cost analysis, the co-fired process ($87/kW) has a similar cost to the multi-fired process ($92/kW). However, the multi-fired process may be technically more attractive because sintering conditions can be tailored to each step.

- Power density
  Power density was kept consistence, which is 470 mW/cm^2 in all scale-up scenarios. The total stack costs based on active area will not be influenced by stack power density.

- Production yield keeps consistence.
  The overall production yield was kept as 75% in all scale-up scenarios. The overall production yield was calculated by accumulating each single process yield. The material

scrap rate was separated from process yield, which is accounted for the material loss in the processes.

4.5. Sensitivity Analysis and Monte Carlo Simulation

A Monte-Carlo-based sensitivity analysis is used early on and throughout the process to maintain an accurate perspective of the model's accuracy and of the uncertainties in the SOFC manufacturing process performance and cost. This type of analysis has proven invaluable in assessing problems with large uncertainty in parameters. It also is instrumental in developing a model refinement plan to establish the statistical significance of differences in manufacturing performance and cost between different approaches.

A third party software package, Crystal Ball, acts as an add-in function in spreadsheet, is used to provide the sensitivity analysis and Monte Carlo simulation. Figure 18 is a sample of the sensitivity analysis output. It illustrates the rank of sensitivity of the parameters to final stack cost.

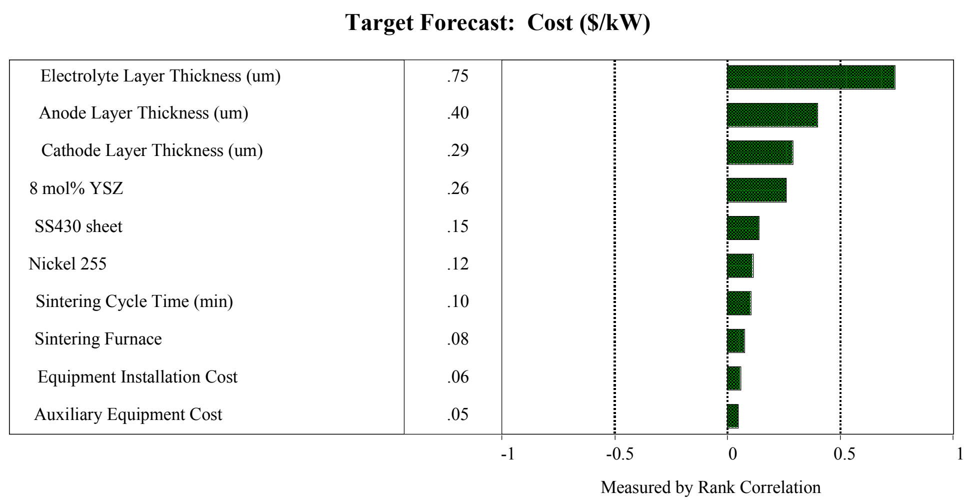

Figure 18 Sample Sensitivity Chart

Figure 19 is a sample frequency chart from the Monte-Carlo simulation, which reveals the total range of the stack manufacturing cost. Each bar on the chart represents the probability of a given stack manufacturing cost. For the assigned parameter uncertainties, this chart shows the statistical probability of a given stack manufacturing cost.

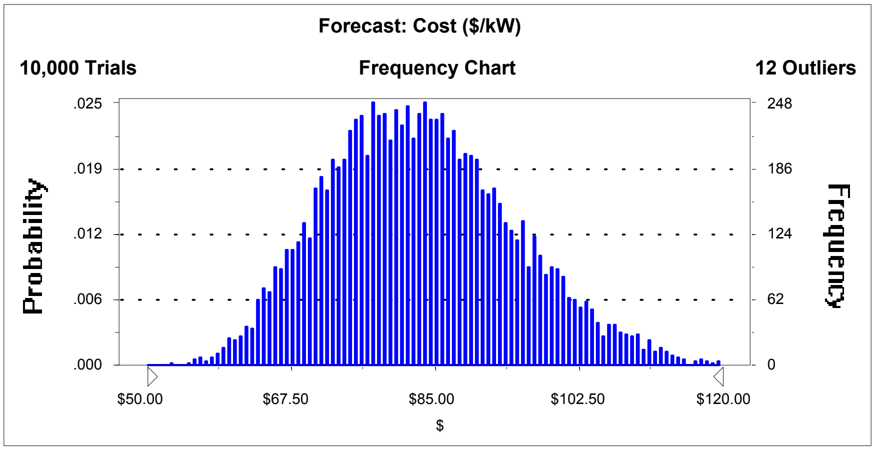

Figure 19 Sample Frequency Chart

4.6. 2003 Model Assumption Summary

4.6.1. Stack Components

Figure 20 shows the stack components and processes included in the manufacturing cost model. Inclusion of stack seals will increase manufacturing process time, yield losses, and material and equipment costs. Sealing and manifolding were not included in this demonstration model.

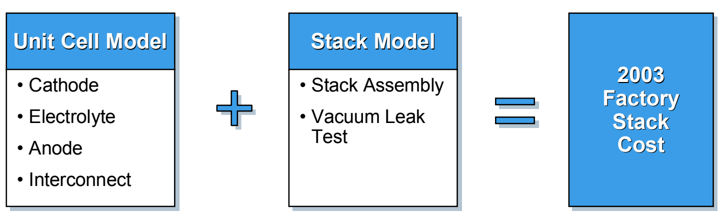

Figure 20 Manufacturing Cost Model Cost Structure

4.6.2. Repeat Unit Layer Thickness

The base EEA layer thicknesses were kept the same as the 1999 study.

Layer	Material	Nominal Thickness (µm)	Remark
Anode	Ni-YSZ	700	• Minimize thickness to reduce material weight and resistance • Impact of thickness on strength and EEA stress
Electrolyte	YSZ	10	• Barrier properties vs thickness critical • Impact of coating technology and thickness on defects
Cathode	YSZ- LSM	50	
Interconnect	Metal	4300	• Roll form technique used in baseline study • Not coated

Table 12 2003 Repeat Unit Layer Thickness

Current EEA practices may utilize more costly designs than assumed for this analysis including:

- Bi-layer electrode structures to enhance 3-phase boundary length and gas diffusion regions leading to additional process steps and costs
- Designers are incorporating additional support layers to reduce ambient temperature bow of the EEA

4.6.3. Related Manufacturing Data

Working Capital	3 Months Mtl + Labor + Utility + Maintenance
Working Capital Period	3 Months
Direct Labor Salary	$35,000 /year
Benefit	35%
Working Day	300 /year
Working Hour	24 /day
Building Rental	$1200 / m^2 year
Price of Electricity	$0.08/kWh
Auxiliary Equipment Cost	80%
Equipment Installation Cost	80%
Misc. Cost	4%
Depreciation	10 years

Table 13 Production Parameters

4.6.4. Baseline Processes

- The anode, cathode, and electrolyte powders are made with ceramic processing steps (e.g., ball milling and calcining)
- Interconnects are made by roll forming of two pieces (anode and cathode flow fields). These are then joined by a brazing process to form the interconnect
- Automated inspection of the layers occurs after sintering, and includes infrared imaging, ultrasonic testing, and vacuum leak testing which checks for helium leaks, dimensions, flatness, and thickness

4.6.4.1. Co-Fired process

The co-fired process steps were the same as the 1999 study with the exception of the electrolyte, where a tape cast layer was replaced by screen printing.

- Tape-cast anode and cathode layers
- Screen printed electrolyte
- Laminated together and co-fired in one step

Additional QC steps were also included.

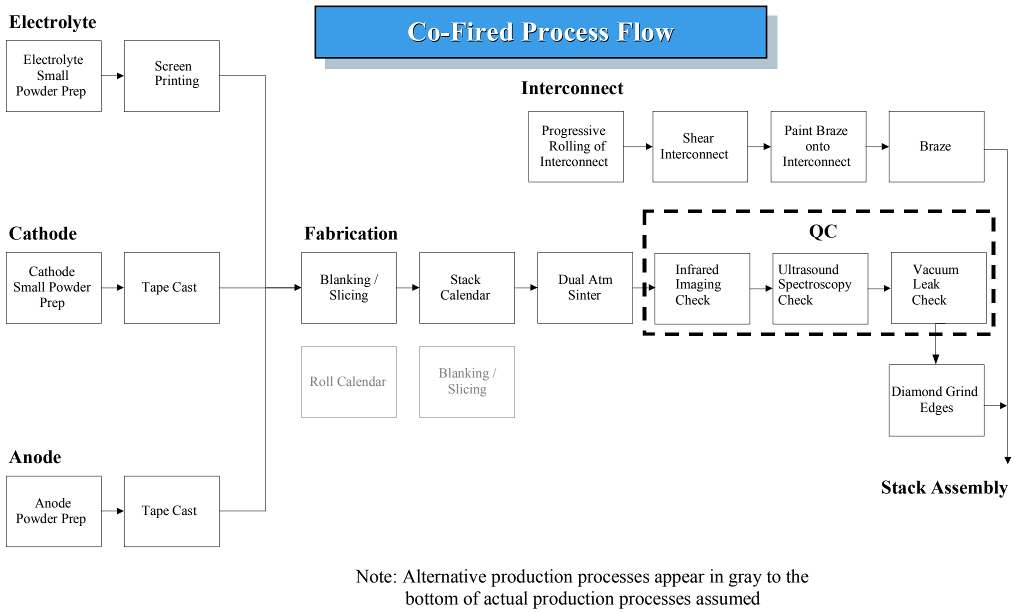

Figure 21 Co-Fired Process Flow Chart

4.6.4.2. Multi-Fired Process

In the multi-fired process, screen printing replaced plasma spray in the electrolyte step and tape casting replaced screen printing in the cathode process.

- Tape-cast anode and cathode layers
- Screen printed electrolyte
- Sequential firing steps

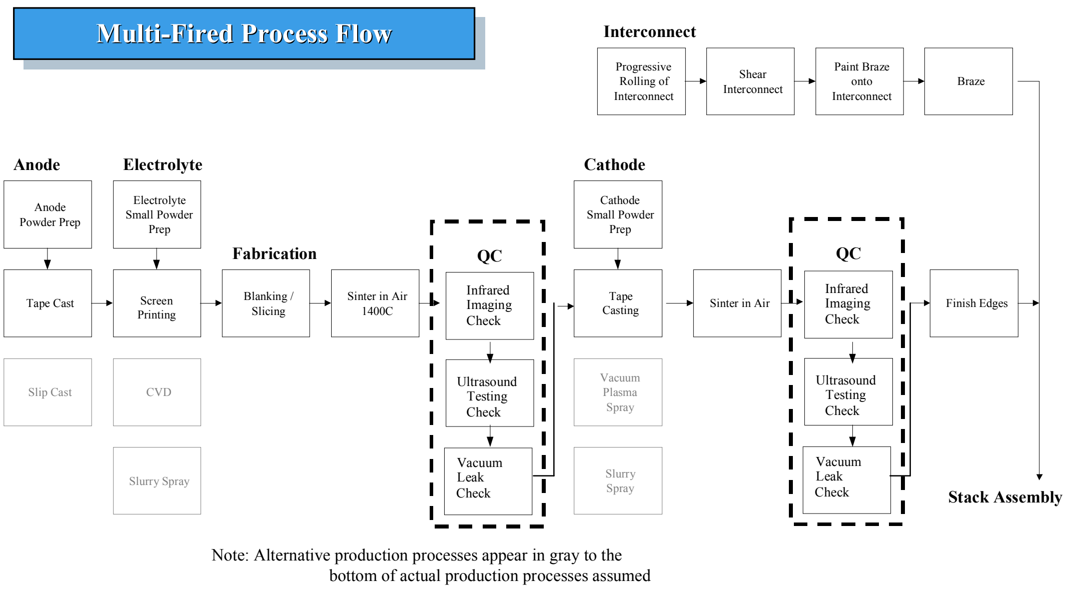

Figure 22 Multi-Fired Process Flow Chart

QC steps were added to the 1999 process after each sinter step.

4.6.5. 2003 Assumption vs. 1999 Assumption

Table 14 summarizes all the assumptions used to calculate the 1999 and 2003 results. The column marked 'sensitivity analysis' shows the parameter range in the 2003 study.

Parameters		1999 Baseline	2003 Baseline	Sensitivity Analysis
Production Volume(MW/Year):		250	250	250
Stack Output(kW):		25	5	5
Size of Cell(cm^2)		100	100	100
Power Density(W/cm^2)		0.5	0.62*	0.72 (Max)*
Anode Thickness(µm)		700	700	300~700
Electrolyte Thickness(µm)		10	10	5~20
Cathode Thickness(µm)		50	50	50~200
Net Voltage Per Tile (V)		-	0.7	0.7
Interconnect Rib Space(cm/rib)		1	0.4	0.4
Production Yield		80%	75%	75%
8 mol% YSZ ($/kg)		$110	$55	$25 ~ $60
LSM ($/kg)		$9	$45	$10 ~ $60
Nickel 255 ($/kg)		$18	$14	$12 ~ $16
Nickel Oxide ($/kg)		$12.90	$10	$8 ~ $12
Anode Process	Co-Fired	Tape Casting	Tape Casting	Tape Casting
	Multi-Fired	Tape Casting	Tape Casting	Tape Casting
Electrolyte Process	Co-Fired	Tape Casting	Screen Printing	Screen Printing
	Multi-Fired	Plasma Spray	Screen Printing	Screen Printing
Cathode Process	Co-Fired	Tape Casting	Tape Casting	Tape Casting
	Multi-Fired	Screen Printing	Tape Casting	Tape Casting

*Calculated from model assuming achievement of low contact resistance

Table 14 Manufacturing Cost Model Assumptions – 2003 vs. 1999

5. RESULTS AND DISCUSSION

5.1. Baseline Cost Results

5.1.1. Performance/Thermal/Mechanical Model

5.1.1.1. Performance Model Results:

In order to determine a baseline power level and manufacturing cost estimate, the performance model was first executed using the nominal layer thickness values listed in Table 15. For the 10-cm square cross-flow cell depicted in Figure 23, an average power density of 470 mW/cm^2 was obtained. The predicted distribution of power density over the active cell area is shown in Figure 23. For the same sized cell operating in co-flow, the predicted power density was 472 mW/cm^2.

Layer	Minimum	Nominal	Maximum
Cathode	50 μm	50 μm	200 μm
Electrolyte	5 μm	10 μm	20 μm
Anode	300 μm	700 μm	2000 μm

Table 15 Range of Layer Thicknesses Simulated

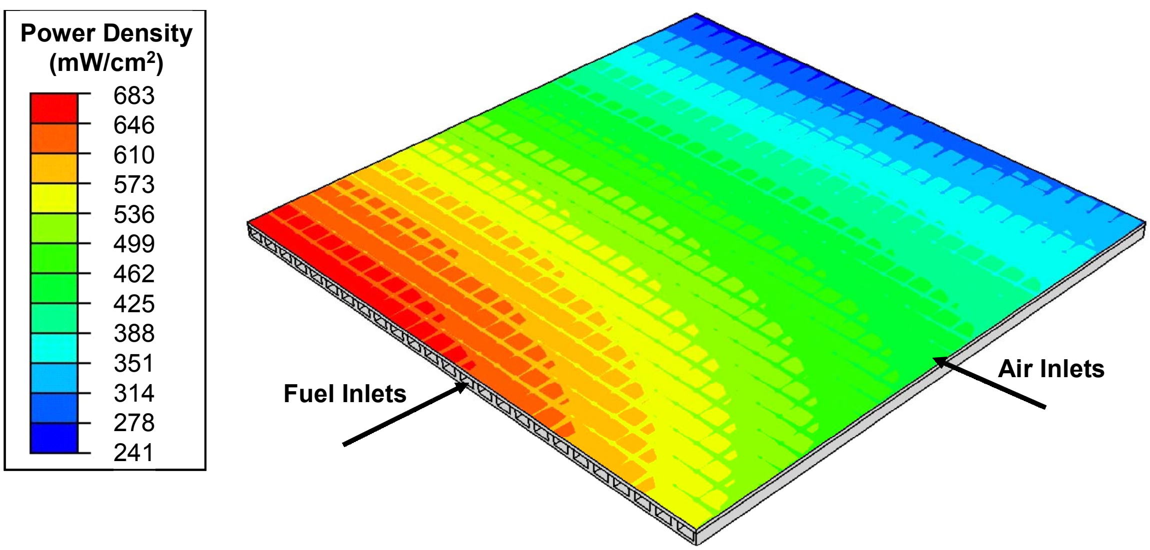

Figure 23 Power Density Distribution of 10 cm Cross-Flow Cell with Nominal Layer Thicknesses and Baseline Operating Conditions, with an Average Power Density of 470 mW/cm^2

We then performed co-flow and cross-flow simulations to determine the sensitivity of the power output to the individual layer thicknesses. Because of the similarity in both trends and absolute magnitude of the results from the two flow configurations, we took advantage of the computational efficiency of the co-flow simulations in obtaining results over the full range of geometries listed in Table 15. A sampling of the calculated values of average power density is given in Table 16.

Anode Thickness (μm)	Electrolyte Thickness (μm)	Cathode Thickness (μm)	Power Density (mW/cm^2)
2000	10	50	345
700	**20**	50	410
700	10	**200**	463
700	10	50	472
700	**5**	50	508
300	10	50	519
300	**5**	50	565

Table 16 Predicted Power Density for selected Combinations of Layer Thicknesses
(Values in bold type deviate from the baseline levels.)

Not surprisingly, the peak power density of 565 mW/cm^2 was obtained at the minimum value of the thickness range examined for each layer, and power decreased with increasing thickness of all layers. Because the cell operating parameters required a high excess air ratio to prevent stack overheating, the electrochemical reaction was never oxygen-starved, and the diffusion through the cathode was not a limiting factor. Therefore, the sensitivity of power density to cathode thickness was minor. In contrast, the diffusion of fuel through the anode was a limitation in the case of thicker anodes, so the anode thickness played a significant role in determining the power output. By far the dominant factor was the electrolyte thickness, because of its major impact on ionic resistance. The dependence of power density on electrolyte thickness is shown in Figure 24 for a range of anode thickness values, at a fixed cathode thickness of 50 μm.

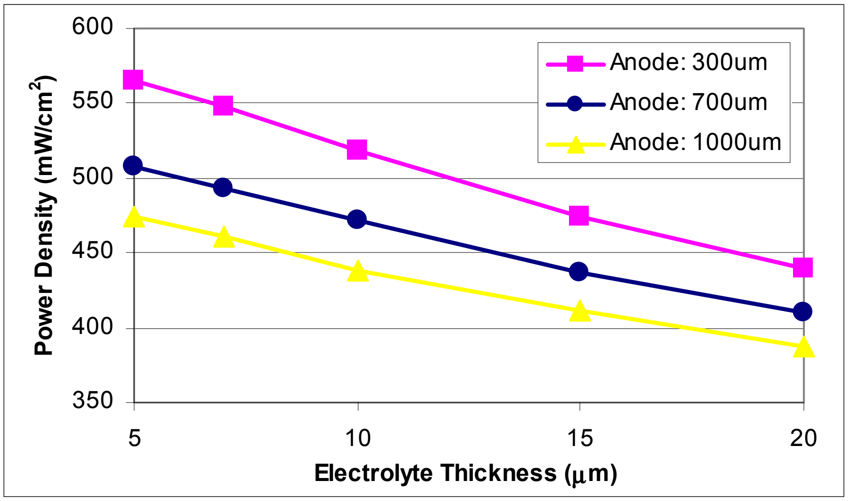

Figure 24 Variations of Cell-Average Power Density at Fixed Nominal Cathode Thickness, Under Baseline Operating Conditions

In order to incorporate these results into the manufacturing cost model, we required a functional form for the dependence of power density on the thickness of each layer. Nonlinear least-squares fitting was used to derive an expression which provides an excellent match to all of the data points obtained using the performance model:

$$P = 603.0 - 0.1336t_a - 8.544t_e - 0.0397t_c + \frac{5001}{t_a} + \frac{116.3}{t_e} + \frac{151.5}{t_c} + 0.003939t_a t_e \,,$$

where P is power density, measured in mW/cm^2, and t_a, t_e, and t_c are the anode, electrolyte, and cathode thicknesses, respectively, each measured in μm. Figure 25 displays the comparison between the functional fit, plotted as a surface, and the predicted data values, shown as 3-D points, for a fixed cathode thickness of 50 μm.

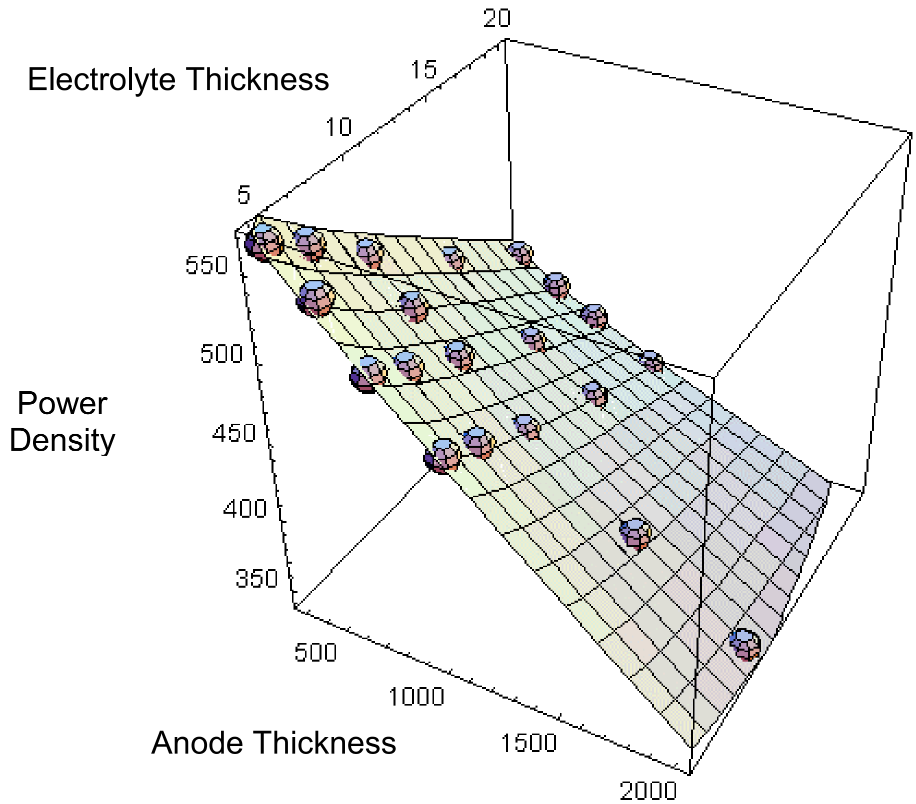

Figure 25 Comparison of Predicted Power Density Values with Best Fit Functional Form, at Fixed Nominal Cathode Thickness
(Symbols represent calculated values and the surface the best fit functional form.)

5.1.1.2. Structure Model Results:

Through finite element analysis of the processing steps and steady-state operation, we determined that the most severe stress state for the EEA occurs during the cool-down from sintering conditions to room temperature, irrespective of the layer thicknesses. During this step, the thermal expansion mismatch among the layers causes a combination of in-plane and bending stresses, with the highest tensile stress at the convex face of each layer. When the EEA is subsequently flattened between interconnect plates, the bending stresses are relieved, reducing the peak stress levels. Finally, when the stack is brought to steady-state operating conditions, the mismatch stresses are relieved further, since the assembly reaches a state closer to the original stress-free condition at the sintering temperature. That is, the steady-state temperature gradients predicted by the performance model are not steep enough to generate thermal stresses as severe as those experienced during processing. On the basis of these conclusions, we focused our attention on the stress state generated during the cool-down steps from sintering conditions.

The thermo-mechanical finite element simulations of processing steps are computationally intensive. Therefore, in order to perform sensitivity studies of the layer thickness effects, we devised a closed-form solution technique for determining the in-plane and bending stresses generated during cool-down. For both the co-fired and multi-fired processes, we obtained analytical expressions for the peak stress magnitude experienced in each layer throughout the processing. Because of the variations in each layer's coefficient of thermal expansion (CTE) with temperature, the peak stress in some cases occurred at an intermediate point between sintering and room temperature. As material failure is governed by the most detrimental conditions experienced throughout the process, these intermediate peak stress levels were captured in the analysis. The closed-form calculations were encoded in an Excel spreadsheet for ease of implementation within the cost model. Using the statistical failure criteria measured at ORNL, material yields were then obtained automatically and incorporated into the final cost estimates. Sample results of peak stress and yield are given in Table 17 for co-fired processing and Table 18 for multi-fired processing.

Case		Thickness (μm)	Peak Stress (MPa)	Failure (%)
Nominal	Cathode	50	45.7	5.1
	Electrolyte	10	-495.2	0.0
	Anode	700	26.6	0.8
Thin	Cathode	50	41.5	3.7
	Electrolyte	5	-493.8	0.0
	Anode	300	27.5	0.9
Thick	Cathode	200	41.5	3.7
	Electrolyte	20	-488.8	0.0
	Anode	1000	31.0	1.4
Mismatch	Cathode	50	71.2	22.0
	Electrolyte	20	-403.0	0.0
	Anode	300	87.6	40.2

Table 17 Predicted Peak Stresses and Material Yields for Co-Fired Processing

Case		Thickness (μm)	Peak Stress (MPa)	Failure (%)
Nominal	Cathode	50	34.1	1.9
	Electrolyte	10	-129.8	0.0
	Anode	700	29.9	1.2
Thin	Cathode	50	31.0	1.3
	Electrolyte	5	-128.2	0.0
	Anode	300	34.9	2.0
Thick	Cathode	200	31.0	1.3
	Electrolyte	20	-125.9	0.0
	Anode	1000	40.4	3.4
Mismatch	Cathode	50	53.1	8.6
	Electrolyte	20	-98.7	0.0
	Anode	300	111.0	69.2

Table 18 Predicted Peak Stresses and Material Yields for Multi-Fired Processing

The stresses that arise during cool-down are driven primarily by the mismatch between the low CTE of the electrolyte and the high CTE of the electrodes. This mismatch forces the electrodes into tension, leading to the possibility of cracking failure. Conversely, the electrolyte is always forced into compression, with no associated chance of fracture. The highest tensile stresses in the electrodes were predicted for the case of a thick electrolyte layer (20 μm) exerting considerably force on a relatively thin anode (300 μm) and cathode (50 μm). Unacceptable failure rates, as high as 69% for the anode in the multi-fired scenario, were predicted for these thickness values, though from a performance standpoint it is unlikely that such a configuration would be attempted. By contrast, minimizing all three layer thicknesses is desirable on both performance and structural grounds, as the predicted stress state is fairly mild and the associated failure rates are below 2% for multi-fired processing. Naturally, this geometry leads to the lowest overall manufacturing cost, as it combines low material requirements, high power output, and acceptable scrap rates.

5.1.2. Manufacturing Costing

For the 2003 model, the co-fired and multi-fired processes continue to be similar in cost, i.e., within 5%, and are $87/kW and $92/kW respectively (Figure 26 and Figure 29). The baseline power density for these values is 470mW/cm^2.

The anode and interconnect dominate the cost contributing approximately 65% of the material and process cost. If coatings are added to the interconnect, possibly doubling its cost, this percentage would increase to 75%.

Total Cost (Materials + Processes) ($/m²)

Co-Fire		$/m2 Material	Process
Process Flow Steps	Anode	$ 123.95	$ 9.63
	Cathode	$ 18.22	$ 7.40
	Electrolyte	$ 6.01	$ 6.18
	Interconnect	$ 118.70	$ 19.25
	Fabrication	$ -	$ 100.99
Sub-Total		$ 266.87	$ 143.45
Total		$410.32	

Multi-Fire		$/m2 Material	Process
Process Flow Steps	Anode	$ 125.92	$ 9.69
	Cathode	$ 14.57	$ 7.07
	Electrolyte	$ 6.11	$ 6.21
	Interconnect	$ 118.70	$ 19.25
	Fabrication	$ -	$ 126.72
Sub-Total		$ 265.29	$ 168.93
Total		$434.22	

Figure 26 2003 Total Stack Factory Cost ($/m²)

Total Cost (Materials + Processes) ($/kW)

Co-Fire		$/kW Material	Process
Process Flow Steps	Anode	$ 26.29	$ 2.04
	Cathode	$ 3.86	$ 1.57
	Electrolyte	$ 1.27	$ 1.31
	Interconnect	$ 25.18	$ 4.08
	Fabrication	$ -	$ 21.42
Sub-Total		$ 56.60	$ 30.43
Total		$87.03	

Multi-Fire		$/kW Material	Process
Process Flow Steps	Anode	$ 26.71	$ 2.05
	Cathode	$ 3.09	$ 1.50
	Electrolyte	$ 1.30	$ 1.32
	Interconnect	$ 25.18	$ 4.08
	Fabrication	$ -	$ 26.88
Sub-Total		$ 56.27	$ 35.83
Total		$92.10	

Figure 27 2003 Total Stack Factory Cost ($/KW)

In this study, cost increased due to higher process costs (primarily added QC steps) and slightly lower power density. The reduced cost of YSZ resulted in lower material costs despite more interconnect material. In the multi-fired process, replacement of the plasma spray electrolyte step with screen printing and higher material utilization lowered the electrolyte cost.

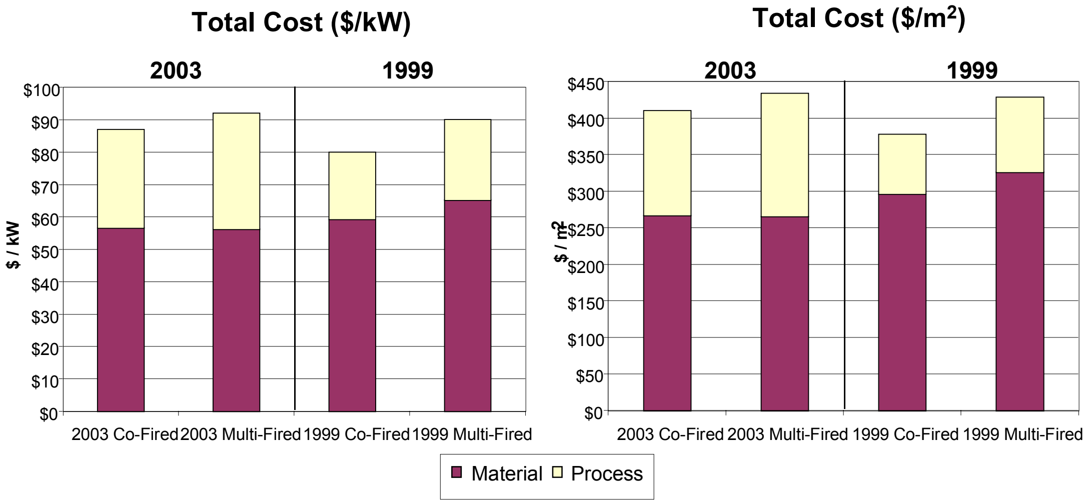

Figure 28 Total Stack Factory Cost Comparison 2003 vs. 1999

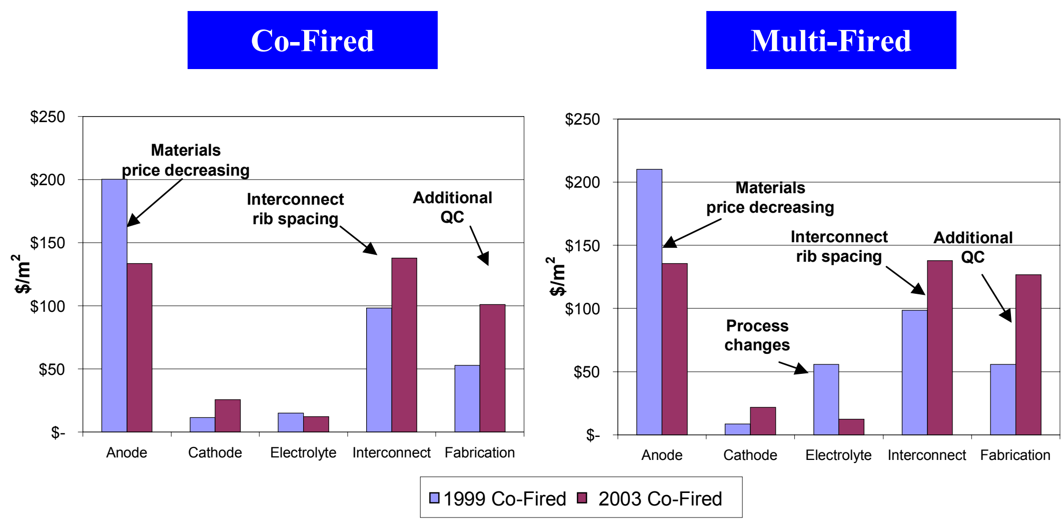

Total Material Cost	Co-Fired ($/m²)	Multi-Fired($/m²)
1999 Model	$378	$429
2003 Model	$410	$434
%Δ	8.5%	1.2%

Figure 29 Total Stack Factory Cost by Layer Comparison 2003 vs. 1999

5.1.2.2. Material Costs

Anode cost dominates the stack because of its mass and material cost. The interconnect cost percentage shown here would be increased because of any functional coatings applied for oxidation resistance and to lower contract resistance.

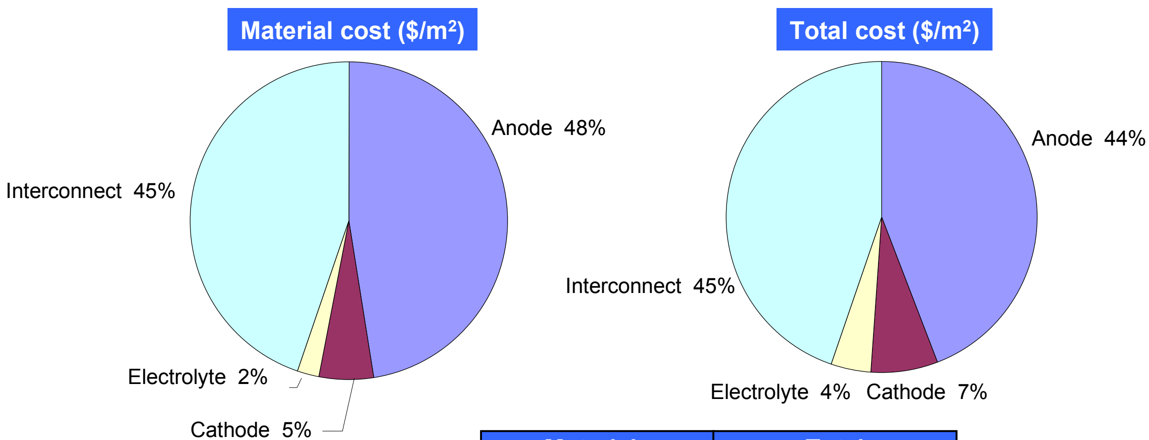

	Materials ($/m²)	Total ($/m²)
Anode	$126	$136
Cathode	$15	$22
Electrolyte	$6	$12
Interconnect	$119	$138

Figure 30 Material Costs Breakdown

In comparison with the 1999 model on an area basis, the 2003 model material cost decreased, largely driven by the reduced 8 YSZ cost. Interconnect cost increased because the rib spacing was reduced from 10 mm to 4 mm to reduce ohmic voltage losses.

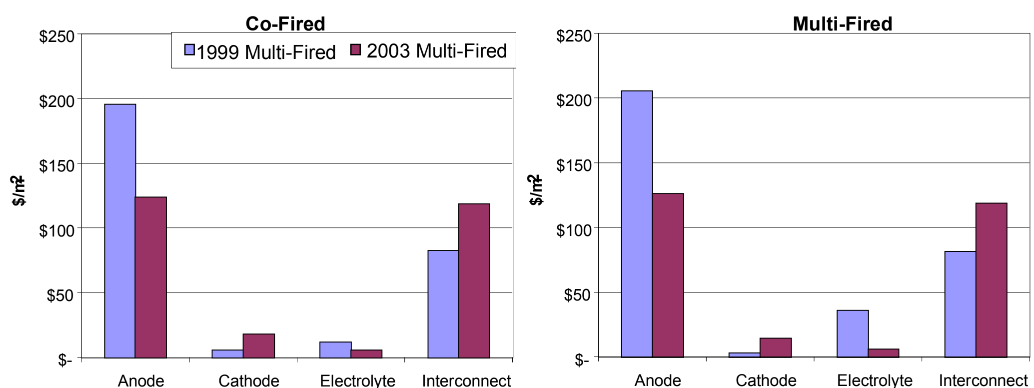

Total Material Cost	Co-Fired ($/m²)	Multi-Fired ($/m²)
1999 Model	296	326
2003 Model	267	265

Figure 31 Material Cost Comparison with 1999 Model

5.1.2.3. Process Costs

Additional QC processes, the final assembly step, and reduced production yield increased the 2003 model fabrication cost by approximately 80 percent.

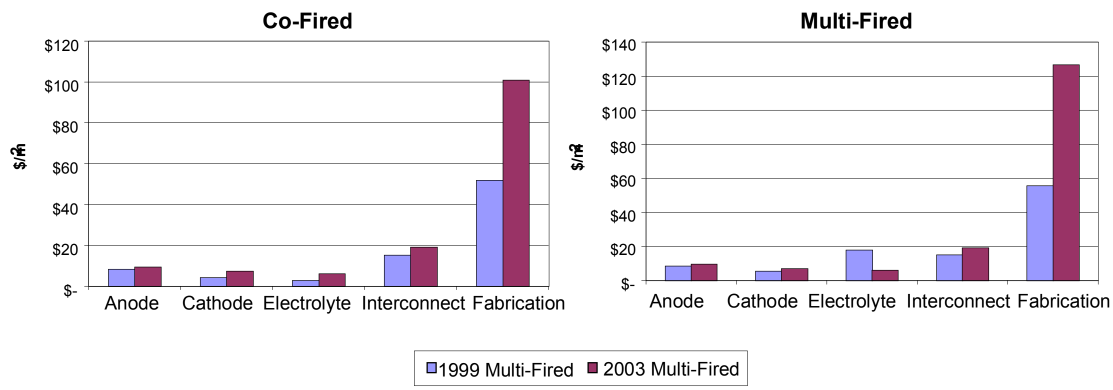

Total Processes Cost	Co-Fired ($/m²)	Multi-Fired ($/m²)
1999 Model	$82	$103
2003 Model	$143	$169

Figure 32 Process Cost by Layer Comparison with 1999 Model

Metal interconnect process costs are the same for both processes and the costs are about $20/m^2$ (not including coating).

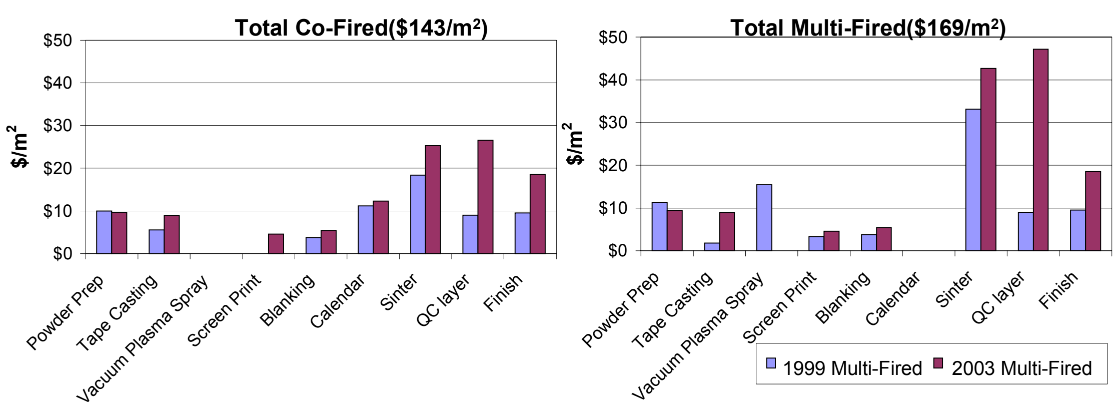

Figure 33 Process Cost by Step Comparison with 1999 Model

5.1.2.4. Manufacturing Cost Analyses

Sensitivity Analysis
Sensitivity analysis shows that the individual layer thickness (Anode, Electrolyte, and Cathode) and YSZ cost are the most important cost factors, as illustrated in Figure 34. The anode is the most important contributor to stack cost and its thickness consequently has significant impact. The electrolyte influences power density and stack cost.

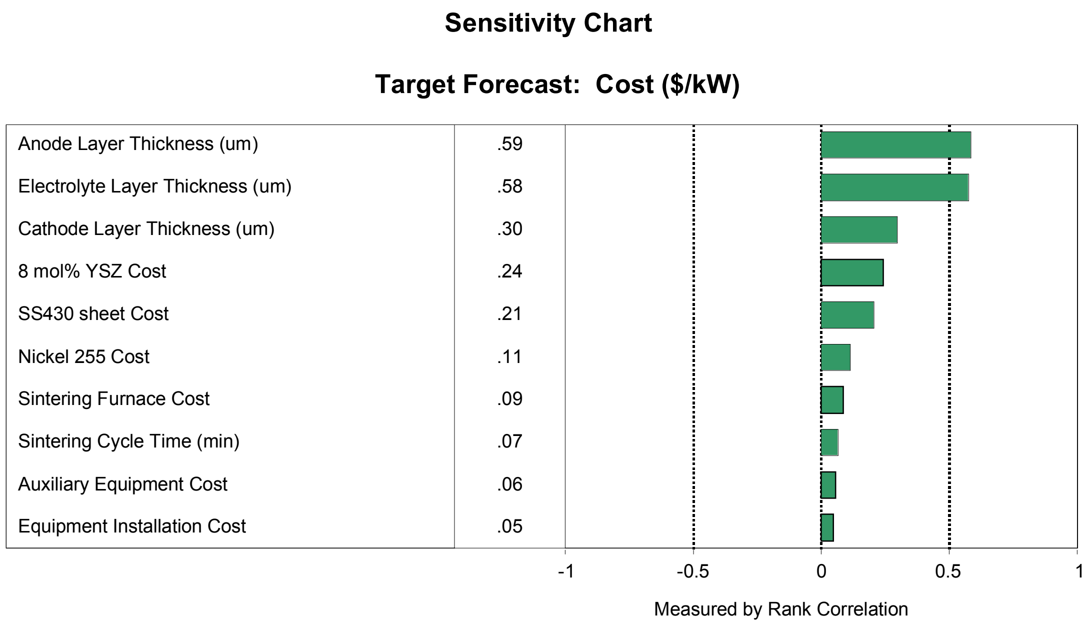

Figure 34 Multi-Fired Process Sensitivity Analysis

Monte Carlo Simulation
Figure 35 shows the results of a Monte Carlo Simulation on Cost for the Multi-Fired process. Given the uncertainty in input parameters, the cost could potentially be as low as $60 /kW or as high as $140 /kW, however, the range of $80 /kW to $120 /kW has 87% certainty.

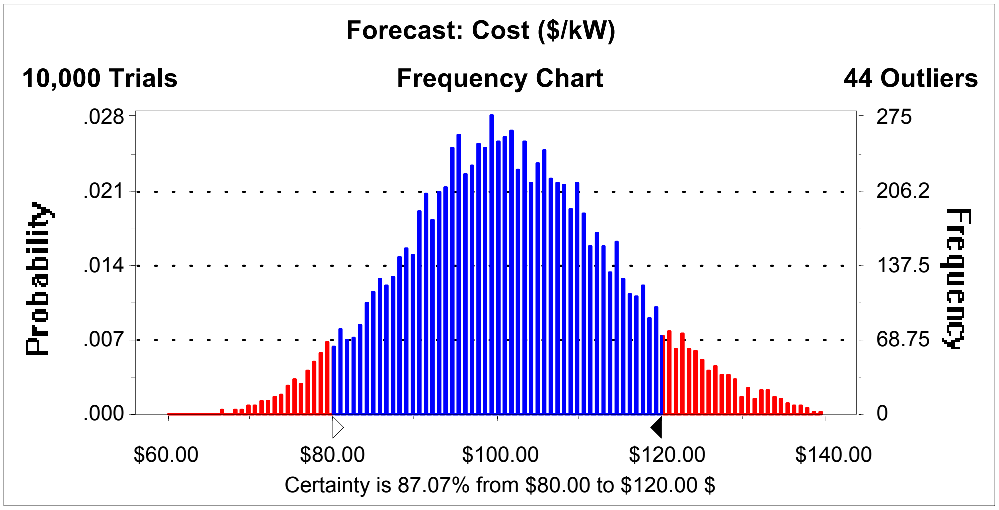

Figure 35 Forecast Frequency Charge from Monte Carlo Simulation

5.2. Economies of Scale

The analysis showed that stack cost reduction is mainly driven by lowering the process cost during production volume scale-up.

Figure 36 and Figure 37 show the stack costs as a function of production volume on a kilowatt basis. The stack cost decreases by 80% by increasing the production volume by 50 times from 5 MW to 250 MW. Over 60% of the cost reduction come at a volume increased of 5 times from 5 MW to 25 MW.

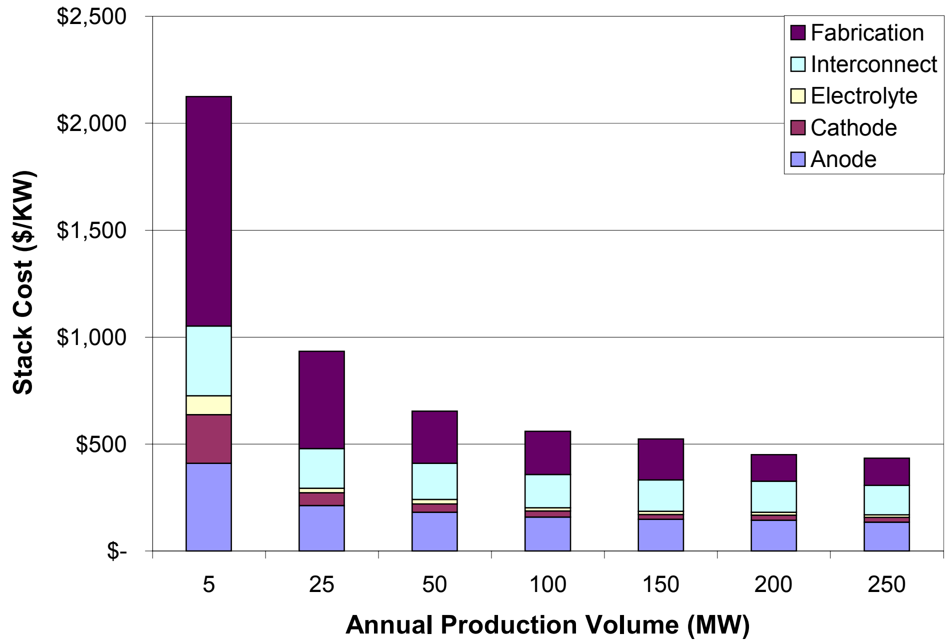

Figure 36 Breakdown Stack Costs as a Function of Production Volume ($\$/m^2$)

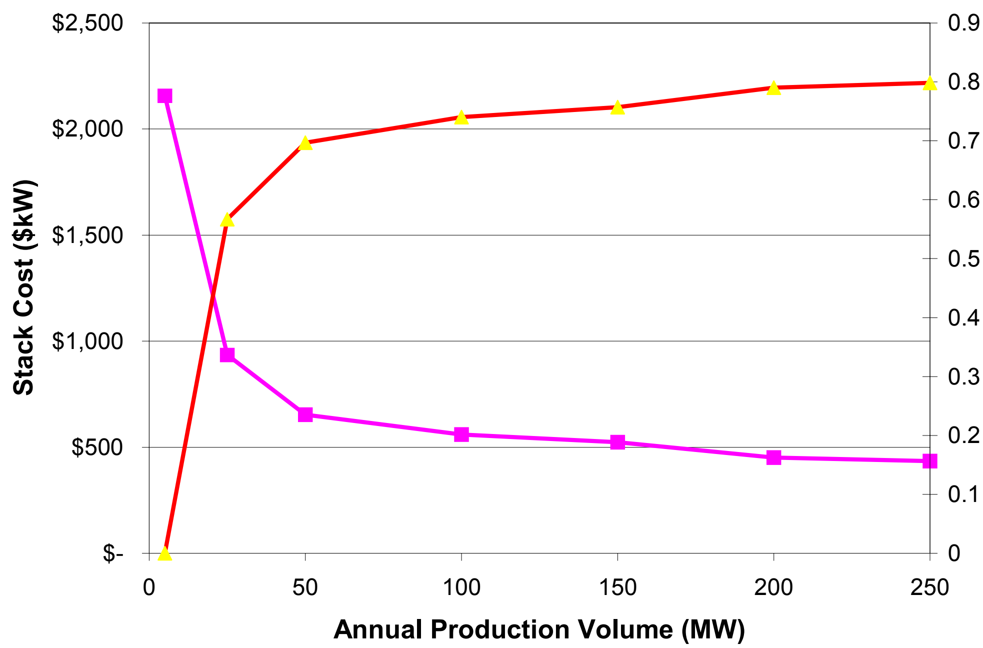

Figure 37 Stack Costs and Cost Reduction Rate as a Function of Production Volume ($\$/m^2$)

As the production volume increases 250 MW, Figure 38 shows that the material cost decreases by 20% and the process cost decreases by 90%.

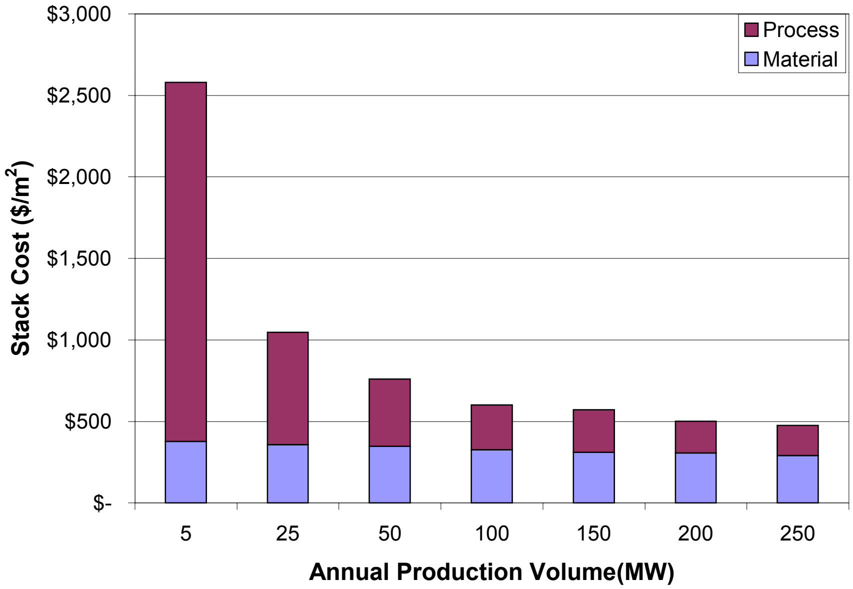

Figure 38 Process and Material Costs as a Function of Productions Volume ($/m^2)

The high cost at low production volumes is caused by high equipment depreciation. To simplify the model structure, it was assumed that the equipment capacity designed for an annual production volume of 25 MW was used for production levels of 25MW or less. Even though small size and manually operated equipment was used, the equipment is still over capacity for production less than 25 MW. It was assumed that equipment cost depreciation is 10 year straight-line. At 5 MW level, the equipment depreciation on each unit will be 5 times higher than the 25 MW level because low production volume can not fill the production capacity.

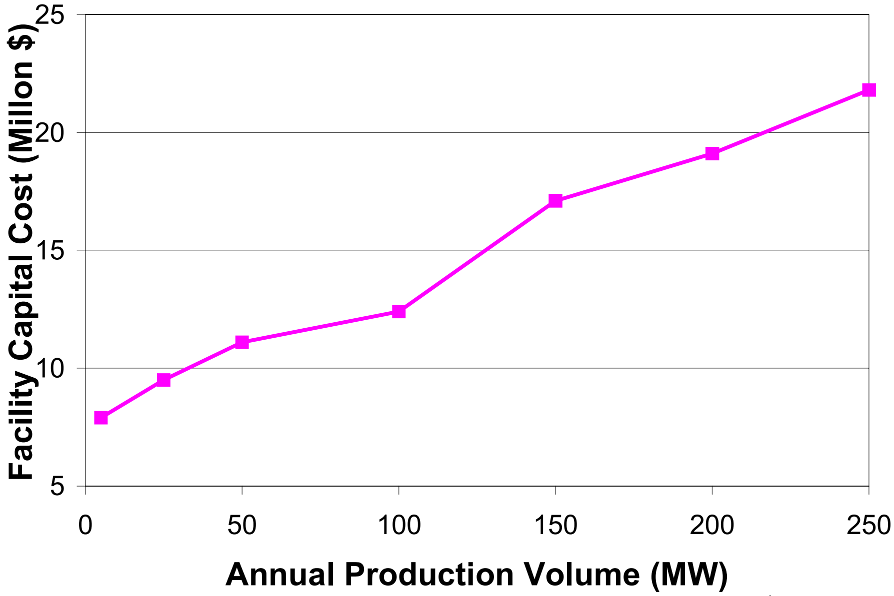

Figure 39 Capital Equipment Cost as a Function of Production Volume (1 Million $)

5.3. Quality Control Analysis Results

5.3.1. Inspection Accuracy Level

In Scenario I added QC steps result in a minimum cost of $92/kW. Scenario II has a higher cost ($118/kW) because defective EEAs & interconnects cause higher process costs, (scenarios described on in Section 4.3.1). These results suggest that more QC inspections distributed through the process will both improve yield while also lowering cost. The accumulated value (materials and process) as the EEAs move through the process is sufficient to justify the cost of the added QC steps.

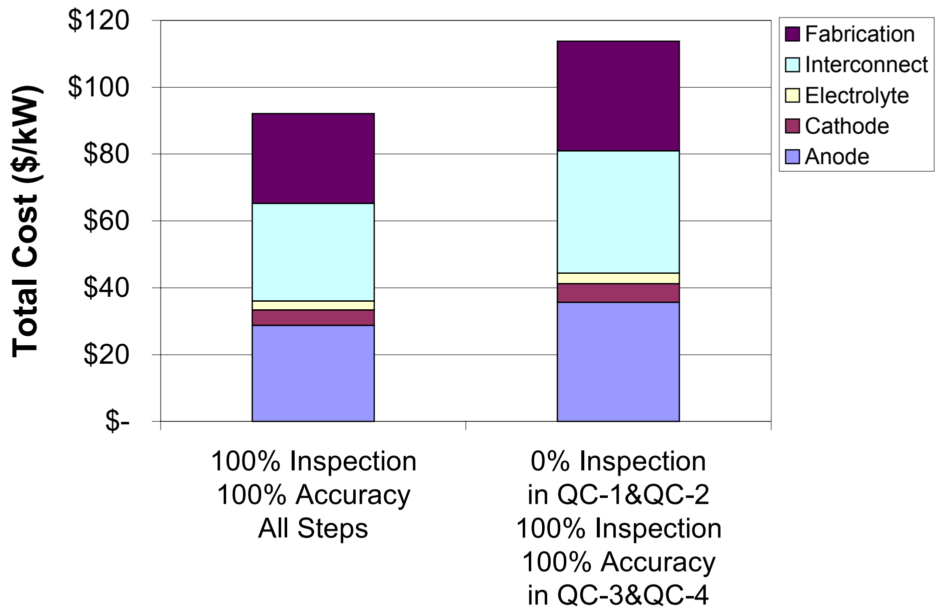

Figure 40 Scenario I & II Total Cost Comparison

5.3.2. Stack Cost vs EEA Defective Rate

For the multi-fired process, stack cost will raise from $92 /kW to $184 /kW if there is the 1% of defective EEAs in the stack.

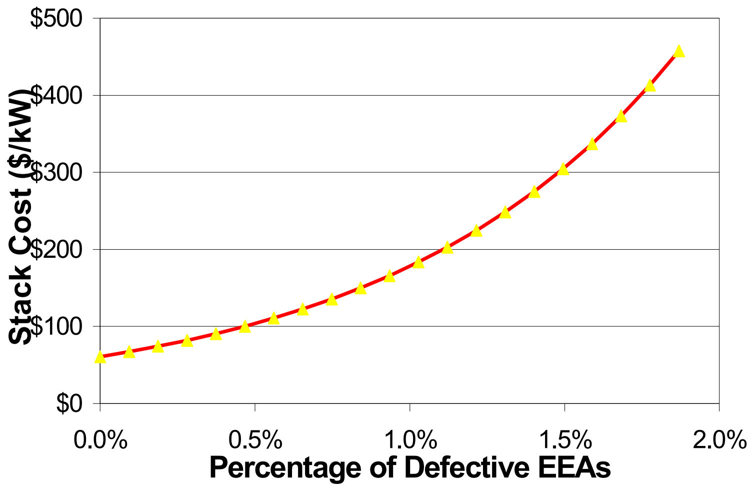

Figure 41 Stack Cost vs. Percentage of Defective EEAs
(number of EEAs, *n*, is 107)

The calculation of stack yield versus percent defective EEAs presented here is only an indicator of the trade-offs between QC inspection costs, selection of stack voltage, and system complexity created from the need for more manifolding and stack-to-stack interconnects as stack voltages are lowered. Performance (current density) and the need for redundancy will also influence the extent to which stacks must be placed in a series/parallel arrangement. The current cost model does not consider the cost of this additional complexity.

5.4. Future Topics for Cost Modeling

The purpose of this project was to demonstrate the capabilities of the cost model and to assess specific manufacturing issues. During discussions with the SECA Teams and NETL other issues for assessment were raised, including alternative production techniques to tape casting and screen printing, coating technologies for interconnects with 3-D flow channels, seal and manifold designs, and balance-of-plant components.

In the current model, we picked tape casting and screen printing as the typical EEA processes, which are less expensive processes compared to sputtering, Chemical Vapor Deposition (CVD), Electrophoretic Deposition (EPD), Electrolytic Deposition (ELD), and Pulsed Laser Deposition (PLD). These deposition processes typically have higher equipment cost and longer cycle time, however, the deposited layer quality is normally higher than less expensive layer deposition processes. Future studies might focus on the tradeoff between cost, quality, and performance of these deposition processes.

Future technology and cost assessments should also target BOP components such as recuperators, blowers, power electronics, stack interconnects, and stack packaging and how system design (e.g., simple or combined cycle), system operating parameters (e.g., temperature and pressure), and fuel (e.g., natural gas, coal gas, or hydrogen) influence the design and cost of these BOP components.

Modeling will provide a framework for capturing critical assumptions and factors and for quantifying the interactions between design technology, selection, and performance assumptions. This needs to be done at the system level to integrate all of the costs.

6. CONCLUSIONS

The updated analysis of stack cost showed that the 1999 cost projections for planar anode supported SOFC stacks should still be achievable ($90/kW). While process costs increased, reductions in YSZ cost offset much of these increases. The addition of Quality Control equipment and procedures in the 2003 model contributed to the increased process cost. Quality control will be critical to successful assembly of stacks with high yields. If defective EEAs pass through final inspections prior to stack assembly at even an one percent level, stack cost could increase by more than a factor of 2 above the baseline projection. Stack voltage will also have an effect on stack yield and limitations on stack voltage will increase the need for series connections of smaller stack and consequently increase system complexity and cost.

Achieving high power densities will be important for decreasing costs due to the large contribution (approximately 85% at high production volumes) of materials to the stack cost. The inclusion of a performance/thermal/mechanical model is important for analyses of this type because real kinetic data, ohmic losses, stack design parameters, mass transport limitations, and temperature gradients can be factored into the projected power density without violating utilization assumptions. Minimization of the thickness of the EEA layers will contribute to increased power density with the electrolyte being the most important factor. In our analysis, the temperature gradient across the stack was limited to 150^{o}C, however, stacks with a higher tolerance to thermal gradients could lead to higher power densities and lower costs.

Significant economies of scale are realized in going from annual production volumes of 5 MW to 250 MW, with approximately 60% of the reduction realized in stepping to 25 MW. For this analysis, reductions in process costs due to higher utilization of capital equipment were a major factor in the decrease in cost.

The SECA Team inputs were important in directing the project efforts to issues critical to SOFC technology development. Going forward, the Teams expressed strong interest in the cost and technology of balance-of-plant (BOP) components such as recuperators, air-handling systems, interconnect components for large arrays of small stacks, and power electronics. At this time, the cost of BOP components contains more uncertainty than the stack and should receive more attention going forward.

Augmentation of the cost model with the performance model provided significant benefit for this analysis, but should provide even more valuable insights in the future as developers consider the tradeoffs between stack operating temperatures, material selection options, and BOP costs.

6.1. Performance/Thermal/Mechanical Model Discussion

The top-level conclusion of the performance and structural modeling is not surprising: to maximize power output and reduce cost-per-kilowatt, one should decrease all layers to their minimum allowable thickness values. However, the models provide significant insight into the effects on performance and cost of adjusting the thickness levels away from the optimum. Deviations from the minimum allowable thicknesses will be driven by considerations external to the simulations such as coating methods, handling and transport during fabrication, and process repeatability. The models can then be used to predict the trade-offs between processing and handling options and performance and structural reliability. The models can also serve as useful tools for evaluating purely hypothetical scenarios, such as the introduction of new active materials, different fuel choices, changes to stack geometry, alternative operating conditions, and so on.

In future work, the cost model can be tailored to the manufacture of specific SOFC designs, however, the performance and structural modules must be modified as well. For instance, the diffusion and electrochemical reaction models can be adjusted to match measured single-cell or stack performance data. The structural model can then be augmented to take into account the stresses generated during handling and transport, edge effects caused by particular seal or manifold designs, and potentially severe thermal gradients experienced during transient operation. Finally, the statistical failure criteria can be improved based on empirical determinations of defect density, material uniformity, fracture strength, and Weibull parameters of the actual chosen SOFC materials.

7. References

[1] J.H. J.S. Thijssen, S. Sriramulu (2002). Assessment of Solid Oxide Fuel Cell Technology, EPRIsolutions, February 2002
[2] E.J. Carlson, S.A. Mariano (1999). Assessment of Planar Solid Oxide Fuel Cell Technology, Arthur D. Little, Inc.
[3] Romero, C. and J.D. Wright (1996). The value and manufacturing costs of planar solid oxide fuel cell stacks, GRI-96/0210
[4] N.Q. Minh, R. Doshi(1999). Preliminary cost manufacturing study for multi-layer thin-film electrolyte solid oxide fuel cells, Honeywell Engines & Systems.
[5] Sossina M. Haile (2003). Fuel cell materials and components, Acta Materialia 51(2003) 5981-6000
[6] Laurel M. Sheppard, (1991). Trends in Milling Equipment, Ceramic Bulletin, Vol.70, No.5
[7] G. Y. Onoda, Jr., L. L. Hench, Ceramic processing before firing, A Wiley-Interscience Publication, John Wiley & Sons.
[8] R. E. Mistler, (1990). Tape Casting: The basic process for meeting the needs of the electronics industry.
[9] J. S. Reed, (1994). Principles of Ceramics Processing, A Wiley-Interscience Publication, John Wiley & Sons.
[10] E. P. Hyatt, (1989). Continuous tape casting for small volumes, Ceramic Bulletin, VOL. 68, NO. 4
[11] H. Ohrui, T. Matshushima, T. Hirai, (1998). Performance of a solid oxide fuel cell fabricated by co-firing, Journal of Power Sources, 71(1998) 185-189
[12] Manufacturing Engineering and Technology, Addison-Wesley Publishing Company Copyright © 1989
[13] ORNL stress study.

8. Appendix

8.1. EEA and Stack Parameters

	Design Parameters	Units
Anode	Anode Layer Thickness	μm
Electrolyte	Electrolyte Layer Thickness	μm
Cathode	Cathode Layer Thickness	μm
Interconnect	Interconnect Thickness	μm
	Interconnect Mtl Thickness	cm
	Desired Rib Spacing	cm/rib
	Actual Ribs per Tile	Rib / Tile
	Rib Height above Flat	cm
	Length of Ribs	cm
	Actual Rib Spacing	cm
	Actual Cross Section	cm^2
Stack	Number of Stacks	Stack / System
	Number of Tiles per Stack	Tile / Stack
	Size of Tile	cm
	Size of Active Area	cm^2
	Pitch	cells/inch
	Stack Height	cm
	Stack Volume	cm^3
	Stack Weight	kg
	System Volume	cm^3
	System Weight	kg
	Net Voltage per Tile	volts
	Stack Voltage	volts
	Net Ampere per Tile	Am
	Net Output per Tile	Watts
	Power Density	mW/cm^2

Table 19 Product Specifications

8.2. Common SOFC Manufacturing Processes

- Wet ball milling

Wet ball milling is a process to prepare the electrode and electrolyte slurries for tape casting, screen printing, and the other forming processes. The milling is done in two stages. In the first stage the milling process breaks down agglomerates and uniformly distributes a deflocculant agent on the ceramic particles. In the second stage, the binder and plasticizers are mixed with the ceramic powders in the mill. The feed material must be within a size range and consistent to control the final particle size. The processing time for tape casting slurry depends on ball mill capacity, load, and slurry characteristics and typically varies from 12 hours to 24 hours. After milling, a de-aeration process usually will be applied to remove the gas in the slurry in a closed vacuum chamber and slurry will be screened to remove any coarse particles. Figure 42 shows the slurry preparation process flow chart.

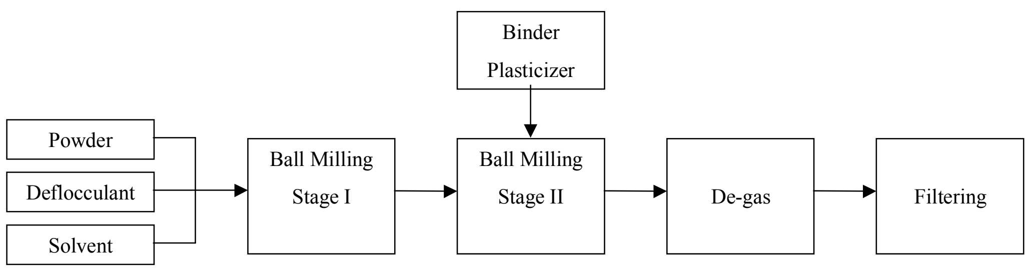

Figure 42 Ball Milling Process

- Tape Casting

Tape casting (Doctor blade casting) is a rapid process of forming ceramic tapes. Tape is made by uniformly spreading slurry onto a smooth surface and then removing volatile solvents. Figure 43 illustrates the main functions of the tape casting machine, which includes the casting head unit, moving conveyor, air-flow drying system, heating system, and tape separation & take-up unit.

Casting head: The casting head is a gate device where the doctor blade can be precisely moved up and down. Dual doctor blades are widely used in industry to control thick tape thickness. The tape layer thickness is controlled by slurry viscosity, moving conveyor speed, doctor-blade setting, and the reservoir depth behind the doctor blade [8].

Moving conveyor: There are mainly three types of carriers, rigid glass plate, continuous steel belts, and flexible plastic film. For rigid glass plate, the casting head moves on the glass. The glass size is normally 150mm to 500mm wide and 1500 mm long [9]. A modern casting machine not only has a continuous stainless steel belt as the moving surface, but also can use flexible film carriers.

Air-flow drying & heating system: The layer of slip is dried slowly on the moving carrier. Heated airflow helps increase the drying speed and solvent vaporizing rate. A viscoelastic, leather-hard tape will be formed at the end of the casting machine.

Tape separation & take-up: Dried tape may be used directly or rolled onto a spool for use in a roll-to-roll process. All types of carrier may be treated with agents to increase release. Silicones, waxes, and soybean derivatives can be applied to the carrier before casting [9].

For industrial tape casting, the casting machine is up to 40 m in length, 1250 mm in width, and a speed up to 1500 mm/min depending upon the drying conditions and production rate. The tape thickness is between 25 μm to 1250 μm [9][10]. After tape casting, punch process is used to apply to get the porous layer.

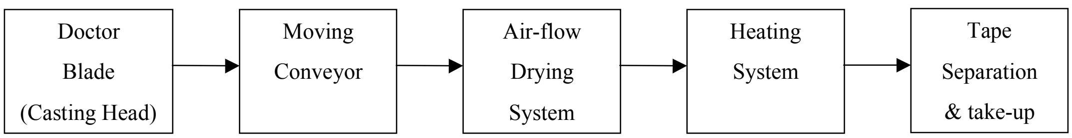

Figure 43 Tape Casting Machine Main Structure

- Screen Printing

Screen printing can be a batch process or a roll-to-roll. It is an inexpensive process compared with sputtering, EVD, CVD processes. In screen printing, a slurry is forced through a mesh to the surface of the substrate by a moving squeegee over the screen. The deposition layer thickness is determined by the diameter of the thread on the screen. The layer thickness is one-fourth to one-third of the filament diameter before drying. It will continue shrink after drying. Typical screen printing thickness is in the range of 2 ~25 μm and the print pattern size is up to 15cm by 15cm. The printing line is as small as 0.25 mm. The squeegee speed is about 25 cm/sec and the cycle time is about 2 second [10]. Figure 44 is the fully automated screen printing batch process flow chart.

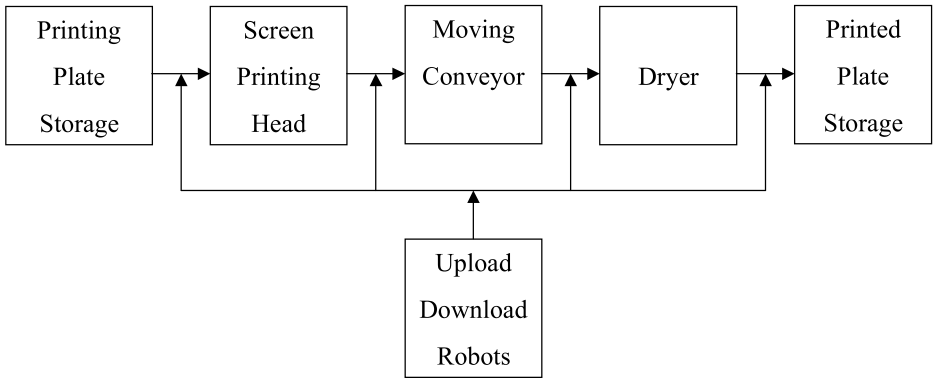

Figure 44 Fully Automatic Screen Printing Batch Process Flow

- Tape Lamination

Lamination is a roll-to-roll process to assemble two or more layers together by high pressure. The lamination pressure varies from 3 to 30 Mpa. After lamination, all layers should be secured together.

- Firing

After material preparation, and forming processes, the anode, electrolyte, and cathode will be fired to product the final product. Firing is one of the most critical steps in manufacturing processes. The heat treatment process will burnout organics, increase component density, shrink the components size, as well as chemical annealing, the three layers of an SOFC stack. Each ceramic material shrinks at a different rate during firing. Also, the anode/electrolyte materials have a different sintering temperature than the cathode material. This makes it a challenge to co-fire the anode, electrolyte, and cathode at the same time. Anode and electrolyte can be co fired together easily and achieve superior performance [11].

- Metal interconnect forming

There are many ways to produce metal interconnects, such as stamping, casting, rolling, etc. The roll forming process uses a series of rolls to progressively form the part. Each rib requires a separate roll. Figure 45 is an example of the roll forming process used to form H-section parts.

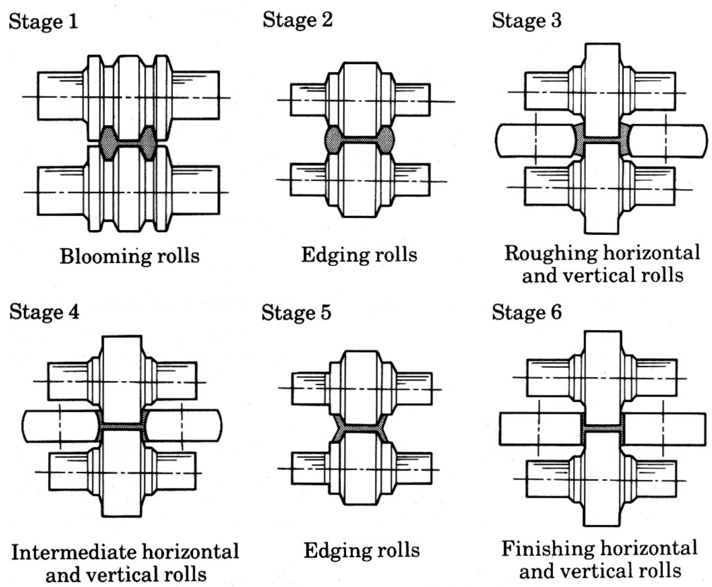

Figure 45 Roll Forming Process Flow

- Other deposition methods

The following deposition methods are possible candidates for electrode layer fabrication.

- Sputtering / Physical vapor deposition (PVD)
- Chemical vapor deposition (CVD)
- Electrochemical vapor deposition (EVD)
- Electrophoretic deposition (EPD)
- Electrolytic deposition (ELD)
- Electrostatic spray deposition (ESD)
- Pulsed laser deposition (PLD)

- Infrared Inspection

Infrared Imaging (IR) is a non-destructive testing method that uses abnormal temperature profiles to indicate a potential problem. IR can be divided into two approaches, the passive approach and active approach. The passive approach tests materials and structures which are naturally at different temperature than ambient while in the case of active approach, an external stimulus is necessary to induce relevant thermal contrasts. We focus on passive approach in this study.

Advantages:

- No contact testing
- Fast inspection rate(up to a few m^2 at a time)

- Results are relatively easy to interpret.

Difficulties:

- Limited thickness of material under the surface.
- Only detecting defects resulting in a measurable change of the thermal properties.
- Effects of thermal losses (connective, radiative) which induce spurious contrasts affecting the reliability of the interpretation.

IR is usually used to detect the cracks on the surface or close to the surface. The cycle time is about 5~8 seconds with automation.

- Ultrasonic Inspection

Ultrasonic Testing (UT) is a non-destructive testing method that uses high frequency sound energy to conduct examinations and make measurements. A typical UT inspection system consists of several functional units, such as the pulser/receiver, transducer, and display devices. A pulser/receiver is an electronic device that can produce high voltage electrical pulse. Driven by the pulser, the transducer generates high frequency ultrasonic energy. The sound energy is introduced and propagates through the materials in the form of waves. When there is a discontinuity (such as a crack) in the wave path, part of the energy will be reflected back from the flaw surface. The reflected wave signal is transformed into electrical signal by the transducer and is displayed on a screen.

Advantages:

- Sensitive to both surface and subsurface.
- The depth of penetration for flaw detection or measurement is superior to other NDT methods.
- Highly accuracy in determining reflector position and estimating size and shape.

Difficulties:

- Linear defects oriented parallel to the sound beam may go undetected.
- Skill and training is more extensive than with some other methods.

UT is usually used to detect the cracks on the surface and under the surface. The cycle time is about 5~8 seconds with automation.

8.3. Economies of Scale Parameters

- Tape casting

	Capex (000's)	Cycle Time (mins)	# of operators per Station	Tooling cost
Manual	$100	0.002	0.5	0
Semi-Automation	$200	0.001	0.3	0
Automation	$300	0.0004	0.2	0

- Blanking /Slicing

	Capex (000's)	Cycle Time (mins)	# of operators per Station	Tooling cost
Manual	$50	0.4	1	$10,000
Semi-Automation	$100	0.2	1	$20,000
Automation	$150	0.17	1	$30,000

- Continuous Sintering (1200^{o}C)

	Capex (000's)	Cycle Time (mins)	# of operators per Station	Tooling cost
Manual	$300	720	0.2	0
Semi-Automation	$400	720	0.2	0
Automation	$500	720	0.2	0

- EEA infrared inspection

	Capex (000's)	Cycle Time (mins)	# of operators per Station	Tooling cost
Manual	$50	0.250	1	0
Semi-Automation	$100	0.167	1	0
Automation	$150	0.083	0.5	0

- EEA Ultrasound inspection

	Capex (000's)	Cycle Time (mins)	# of operators per Station	Tooling cost
Manual	$20	0.250	1	0
Semi-Automation	$70	0.167	1	0
Automation	$150	0.083	0.5	0

- EEA vacuum leak test

	Capex (000's)	Cycle Time (mins)	# of operators per Station	Tooling cost
Manual	$100	0.50	1	0
Semi-Automation	$200	0.33	1	0
Automation	$300	0.17	1	0